COO-2679-8

CONF-761027--13

VACANCY DEFECT MOBILITIES AND BINDING ENERGIES OBTAINED FROM ANNEALING STUDIES†

R. W. Balluffi

Department of Materials Science and Engineering
and Materials Science Center
Cornell University, Ithaca, New York 14853

November 1976

Cornell University
Ithaca, NY 14853

Report #2761

Issued by

The Materials Science Center

† Prepared for presentation at the International Conference on the Properties of Atomic Defects in Metals, Argonne National Laboratory, Argonne, Illinois, 18-22 October, 1976.

DISCLAIMER

ABSTRACT

A review is given of our current knowledge of the mobilities and binding energies of vacancy defects in a number of FCC and BCC metals (i.e., Cu, Ag, Au, Pt, W and Mo) as derived from annealing experiments after quenching and/or irradiation. It is concluded that vacancy defects are retained by quenching in all of these metals, and that Stage III annealing after irradiation occurs by the migration of vacancy type defects. The annealing process after quenching is potentially complex and in Au and Al may involve at least mono- , di-, and tri-vacancies. Annealing in Stage III after irradiation can also be complex and involve at least mono- and divacancies. Great difficulties are therefore involved in extracting reliable defect properties from such experiments. The monovacancy migration energies derived from annealing experiments after both quenching and irradiation are in reasonably good agreement for most of the metals. Also, the sum of the monovacancy migration energy and the formation energy is in reasonable agreement with the activation energy for self-diffusion due to monovacancies. The temperature of Stage III annealing after irradiation is generally lower than the temperature of the annealing after quenching because of a smaller number of defect jumps to annihilation in the former case. The limited available information about divacancies in the FCC metals indicates that they possess binding energies in the range 0.1 - 0.3 eV and migrate more easily than monovacancies. The even more limited information about trivacancies in Au and Al indicates that they are at least as mobile as divacancies and are rather loosely bound. No comparable information about divacancies and trivacancies in the BCC metals is yet available.

1. INTRODUCTION

In the present paper we review current knowledge of the mobilities and binding energies of vacancy defects in a number of metals as derived from annealing experiments after quenching and/or irradiation. As is well known, such annealing experiments often involve complex phenomena which are difficult (and sometimes impossible!) to interpret unambiguously on the basis of the information at hand. Therefore, despite a large effort extending over more than 20 years, our knowledge of certain basic defect properties is still rather limited and in some cases controversial. However, considerable progress has been made in the last few years, particularly as a result of the introduction of new experimental techniques, and a number of important results now seem well established. Extensive reviews of previous work may be found in the proceedings of the conferences held at the Argonne National Laboratory in 1964[1], at Jülich in 1968[2,3], at Mol in 1971[4], at Sussex in 1972[5], at Gaithersburg in 1973[6], and most recently at Gatlinburg in 1975[7].

We shall restrict ourselves mainly to the information which can be extracted from annealing experiments after quenching and/or irradiation, and we shall not consider in any significant detail other defect related phenomena which are taken up elsewhere in this Conference. Furthermore, we shall consider only the FCC metals Cu, Ag, Au, Al and Pt and the BCC metals Mo and W. These groups of metals possess close packed and non close packed structures respectively and also exhibit a range of electronic structures. Also, each metal has received at least a fair amount of attention experimentally.

2. ANNEALING OF VACANCY DEFECTS IN QUENCHED SPECIMENS

2.1 Introductory Comments

It is now well recognized that the annealing process after (or during) quenching can be exceedingly complex[8-21]. In many cases effects due to the simultaneous annealing of several mobile defects, e.g., monovacancies, divacancies, trivacancies,

etc., are measured under conditions where the concentration of each species cannot be monitored individually[9,12,14,16]. Great care must therefore be taken if attempts are made to derive vacancy defect binding energies and mobilities from the macroscopically measured kinetics. Difficulties may arise from a variety of sources which include:

(1) unknown distributions of defects produced by quenching and/or annealing as a result of losses to sinks, reactions between defect clusters, etc. [9,14,19-21].

(2) time dependent sink densities and configurations[9,19]. For example, the nucleation and growth of vacancy precipitates (sinks) may occur during the annealing.

(3) sink efficiencies which may be both defect supersaturation and temperature dependent[9,17,19-22].

(4) effects due to defect-impurity interactions[17].

(5) interaction effects due to the stress fields of the annealing defects and the sinks[17].

(6) problems in interpreting effective migration energies, particularly as determined by the change-of-slope method[9,10,18-21]. In this method transients in the quasi-steady state defect populations caused by the rapid temperature change may produce misleading effective migration energies.

The potential difficulties which are involved are particularly well illustrated by the computer simulation studies of Johnson[12] of the annealing and clustering of vacancy defects in a general system in which clusters of up to seven vacancies were explicitly treated and where reasonable approximations were made to account for larger clusters. He concludes that the resulting annealing curves often give little indication of the actual defect processes occurring and that the input data (defect parameters) usually cannot be inferred from standard analyses of isothermal and isochronal data.

Despite these difficulties many efforts, e.g., [11,18,23-26], have been made to interpret annealing data on the basis of a relatively simple mono-, divacancy annealing model in which it is assumed that the rate limiting step is the diffusion rate of these interacting defects to sinks. A number of investigators, e.g., [9,11, 19-21,27], have also employed a more complex mono-, di-, trivacancy model in the interpretation of certain data. The most extensive investigation of the general behavior of the mono-, di-, trivacancy model has been carried out by the group at Stony Brook[19-21]. By the use of computer simulation they have investigated the nature of the defect distribution which is frozen out during quenching and the important question of the degree with which mono-, di-, and trivacancies are able to maintain equilibrium with each other as they anneal to sinks. Their results[20] indicate that temperature, defect concentration and sink density are important parameters, as might be expected, and that the common assumption of local equilibrium is not always valid under real annealing conditions except in cases of relatively low sink densities and high annealing temperatures.

In the light of the above remarks we may expect to find considerable differences in the annealing behavior reported in the literature by different investigators. For example, the vacancy defect precipitation leading to the formation of sinks is usually heterogeneously nucleated at impurities[28]. Therefore, subtle differences in impurity concentrations in the specimens used by different investigators may have radically affected the sink structure which in turn would have influenced the possible attainment of equilibria between the migrating defect populations and the resulting overall annealing rate. We may therefore expect to find differences between the values of the defect parameters reported by certain investigators. In many of the experiments reported in the literature little, or no, information was available concerning the sink density and structure, and other physical parameters which might have affected the kinetics were often unknown. In certain cases oversimplified models have undoubtedly been applied in order to achieve apparent fits with data obtained over narrow ranges of annealing conditions.

In the following we discuss the results obtained for each metal and attempt to identify the most reliable values of the defect properties.

2.2 Results of Quenching Experiments

2.2.1 gold

The mobile vacancy defects in quenched Au anneal out in one main annealing stage located somewhere in the temperature range 300-450 K as seen in Fig. 1a[29-39].† In this stage the vacancy defects either annihilate at fixed sinks or else form large immobile clusters which eventually anneal out in a further discrete annealing stage located at a considerably higher temperature, i.e., >700 K [27,30, 31,35,40]. The immobile sink clusters are evidently nucleated at small concentrations of certain impurities in the ppm concentration range, and large variations in sink density have therefore been observed[41,42]. The temperature of the annealing stage, T_a, decreases as the concentration of quenched-in defects increases (Fig. 2a). The annealing peaks, determined by isochronal annealing, are generally wider than would be expected for a single thermally activated process. All of the peaks observed to date, with the exception of those observed by Dawson and Das[36], appear structureless. The latter peaks, which were determined with particular care, possess a substructure indicating the possible presence of at least three partially overlapping subpeaks (Fig. 3a). Corresponding isothermal annealing curves generally have complex shapes, e.g., [19,41,42], and only occasionally follow simple kinetic laws, e.g., [23]. In addition, effective migration energies determined in different regions of defect concentration and temperature by a variety of techniques[9,18] possess values ranging from as low as 0.5 eV[18] to as high as 1.0 eV[24]. The above results all indicate an annealing defect system in quenched Au in which several mobile and interacting defect types may be present simultaneously and where the defects often anneal to sinks produced by the precipitation of the defects.

† No effort has been made in Fig. 1a (or in the following figures) to normalize the data to a standard defect concentration or isochronal annealing schedule.

What appear to be the best characterized annealing experiments in Au have been carried out very recently by the group at Stony Brook[19-21]. In this work vacancy defect annealing to fixed sinks consisting of a distribution of already established and completely characterized vacancy clusters (stacking fault tetrahedra) was studied under conditions where no further cluster nucleation occurred. Effective migration energies were obtained by comparing quasi-steady state annealing rates, and therefore transient effects due to sudden temperature changes were avoided. Furthermore, the sink efficiencies of the stacking fault tetrahedra were known from the results of earlier experiments[22] which had shown that the efficiency possesses an effective activation energy of 0.07 eV due to the presence of a growth barrier which must be overcome when vacancy defects are destroyed at a tetrahedron. Effective activation energies for the annealing were determined in the temperature range 21-85°C, and the results (after corrections were made for the temperature dependence of the sink efficiency which decreased the observed energies by 0.07 eV) are shown in Fig. 4. Also included in Fig. 4 is a cross-hatched band which defines the loci of a large number of data points obtained by a number of other investigators[25,35,41-43] over the same range of temperature and total defect concentration. (These latter data points have also been corrected for the temperature dependence of the sink efficiency.) Finally, "instantaneous" effective activation energy data obtained by Burton and Lazarus[18] using a continuous resistivity measuring technique and an instantaneous change of slope method are also included. No corrections were applied to these data, since presumably the "instantaneous" effective activation energies do not include the effective activation energy corresponding to the growth barrier at the sinks[18]. The results are seen to be in reasonable agreement with the exception of a few of the Burton-Lazarus data points which appear low. We note that the application of the sink efficiency correction has markedly improved the agreement between the data. Attemps[21] made to fit the data to a mono-, divacancy model using computer simulation were unsuccessful, and it was found necessary to employ a mono-, di-, trivacancy model. Ranges of values of the migration and binding energies of the three defect types consistent with the

observed annealing kinetics, available self-diffusion data and available equilibrium vacancy defect concentration data are given in Table 1. In general it was not possible to determine unique values of all of the parameters involved which include entropies, frequency factors, etc., since it was found that a large number of sets of parameters possessing slightly different individual values fit the observed data almost equally well. Values chosen within the limits given in Table 1 are therefore highly correlated. One specific set of defect parameters which were found to fit the data is the following: $E^f_{1v} = 0.94$ eV, $S^f_{1v} = 0.72$ k, $E^m_{1v} = 0.85$ eV, $E^b_{2v} = 0.32$ eV, $S^b_{2v} = -1.00$ k, $E^m_{2v} = 0.70$ eV, $E^b_{3v} = 0.52$ eV, $S^b_{3v} = -1.50$ k, $E^m_{3v} = 0.53$ eV, $D^\circ_{1v} = 4.55 \times 10^{-2}$ ($cm^2 s^{-1}$), $D^\circ_{2v} = 4.18 \times 10^{-4}$ ($cm^2 s^{-1}$) and $D^\circ_{3v} = 2.09 \times 10^{-4}$ ($cm^2 s^{-1}$). In the course of fitting the data the entire quenching and annealing process was simulated, and it was found that the defect populations were in approximate local equilibrium with each other under the conditions of the experiment.

These results are of considerable interest since they indicate that a mono-, di-, trivacancy model is required to explain much of the Au annealing data. Furthermore, the results (Table 1) are consistent with a relatively loosely bound trivacancy which is more mobile than the divacancy which in turn is more mobile than the monovacancy. It is interesting to compare this result with the isochronal annealing data in Fig. 3a where the three observed sub-peaks labeled A, B and C may be due to mono-, di- and trivacancies respectively as originally suggested by Dawson and Das[36]. The decrease in T_a with increasing T_q seen in Fig. 2a is readily explained by increases in both the effective defect mobility and the sink density as the defect concentration increases.

The divacancy migration energy in Table 1 is in apparent agreement with the value of 0.68 eV obtained by Franklin and Birnbaum[44] by use of anelastic measurements. However, certain aspects of these anelastic measurements are not clearly understood[45].

A somewhat disappointing aspect of the above results is the relatively poor resolution achieved in the determination of the individual defect parameters

(Table 1). Jain and Siegel[19] mention that the situation would be much improved if data at higher annealing temperatures were available. Kino and Koehler[24] and Sharma, et al.[46] obtained effective migration energies in the range 0.9 eV for annealing temperatures near 150°C. However, Sharma, et al.[46] point out that when the quenching rate was reduced, migration energies near 0.69 eV were obtained. They suggest that these results may have been due to possible differences in the sink densities. Jain and Siegel[19] discuss other high temperature data which are found to be generally unsatisfactory.

Numerous other quenching studies have appeared in the literature, and many of these have been reviewed elsewhere[8,11,13]. As pointed out in [41] a number of these appear to be reasonably consistent with the results shown in Fig. 4. However, others show apparent inconsistencies. In these cases, insufficient information is generally available to allow a clearcut interpretation of the results, and we therefore shall not pursue these experiments further.

2.2.2 aluminum

The mobile defects in quenched Al anneal out in a main annealing stage located between about 200 and 350 K [47-57] as indicated in Fig. 5a. As in Au, the defects either anneal to fixed sinks or to defect clusters which in turn anneal out in a further discrete stage at a higher temperature (Fig. 5a). Also, T_a tends to decrease as the defect concentration, i.e., T_q, increases (Fig. 2b). The density of the defect clusters formed is usually sensitive to impurities[28] as in Au, and this probably accounts for much of the data scatter in Fig. 2b. In the early work the isochronal annealing peaks for this main stage appeared structureless, but when higher purity samples were used, a clearly resolved substructure was detected[49,53,54,56] as seen, for example, in Fig. 3b. The substructure consists of two peaks, A and B, spaced ~70 K apart. At high defect concentrations (high T_q) the low temperature peak A dominates whereas at low defect concentrations (low T_q) the high temperature peak B dominates. Measurements in [56] indicate that the activation energy for the

annealing in peak B is 0.65 eV which is associated with a simple process corresponding to monovacancy migration. On the other hand, the annealing in peak A is not simple and possesses an effective activation energy ranging between 0.44 and 0.50 eV. The overall picture which emerges is that of a system where monovacancies are the dominant defects annealing at the low concentrations but where more mobile clusters become important at the high concentrations. As in Au, the decrease in T_a with increasing T_q seen in Fig. 2b may be attributed to increases in both the effective defect mobility and the sink density as the defect concentration increases. Levy, et al.[58] attempted to fit these data by computer simulation using a mono-, divacancy model without success. However, a good fit was obtained with a mono-, di-, trivacancy model in which the divacancy is more mobile than the monovacancy, and the trivacancy is at least as mobile as the divacancy. Again, as in the work of the Stony Brook group with Au [Section 2.2.1], the entire quenching and annealing process was simulated so that the behavior of the different defect populations was evaluated at all times. The values of the derived defect parameters are given in Table 1.

These results are generally consistent with results obtained in a number of earlier and less detailed investigations. There is general agreement that divacancies play an important role in the annealing, and that $E^m_{2v} \sim E^m_{1v}$. DeSorbo and Turnbull[59] first found that monovacancies tend to dominate the kinetics at very low defect concentrations and found $E^m_{1v} = 0.65$ eV. At intermediate concentrations at least monovacancies and divacancies are important, and Doyoma and Koehler[48] obtained $E^m_{2v} = 0.50$ eV and $E^b_{2v} = 0.17$ eV from a consideration of monovacancy and divacancy contributions. Federighi[49], Kiritani, et al.[60] and Roebuck and Entwistle[55] found evidence that monovacancy migration can evidently also control the rate of annealing at very high concentrations but under quite different conditions were the rate limiting step is now the diffusion together of monovacancies to form divacancies which in turn diffuse rapidly to sinks.

2.2.3 platinum

A single annealing stage, without detectable substructure, is observed in Pt[61-66] in the temperature range 600-760 K as indicated in Fig. 6a. As usual, T_a tends to decrease as the concentration of quenched-in defects is increased[61-66]. As Jackson points out[61], the residual resistivity of any vacancy clusters remaining after the mobile defects have annealed is far less than in, for example, Au.

The information about the defects which can be obtained from the available annealing experiments is less satisfactory than for the previous cases of Au and Al. However, most of the results appear to be consistent with an annealing system in which the effects of highly mobile clusters become important at high defect concentrations just as in Au and Al. Ascoli, et al.[67], Bacchella, et al.[68] and Jackson[61] found E^m_{eff} values of 1.42, 1.48 and 1.38 eV respectively at low concentrations (low quenching temperatures), whereas Bacchella, et al.[68], Piercy[69] and Jackson[61] found values of ∿1, 1.13 and 1.10 eV respectively at high concentrations (high quenching temperatures). Polak[63], in a more systematic study, found that E^m_{eff} decreased with an increasing defect concentration or a decreasing annealing temperature. Schumacher, et al.[64] also obtained results indicating a relatively high activation energy, 1.33 eV, at low defect concentrations, and a lower energy, ∿1 eV, at higher concentrations. On the other hand, Rattke, et al.[65] reported that either low or high E^m_{eff} values (independent of defect concentration) could be obtained depending upon the sink density. They suggested that these results were due to interactions of the defects with the sinks. However, this explanation seems unlikely. We note that the E^m_{eff} values in this work were derived by questionable methods, and the significance of these results is therefore difficult to judge. Finally, Berger, et al.[70] observed the individual vacancy defects quenched into Pt (T_q = 1700°C) directly by field ion microscopy. They found 157 monovacancies and 9 divacancies in 593,800 sites in three as-quenched specimens and 76 monovacancies and 1 divacancy in 321,300 sites in five specimens which were partially annealed after quenching. By considering the behavior of the mono- and divacancy populations

during quenching, and assuming that $E^m_{1v} = 1.38$ eV, they derived a value of $G^b_{2v} = 0.23$ eV for the divacancy binding free energy at 443°C. The preferential loss of divacancies in the partially annealed specimens provided important direct evidence that the divacancy is indeed more mobile than the monovacancy.

The values of the defect parameters derived by the above investigations from the various experimental results differ somewhat, and all are subject to certain uncertainties. These include, for example, the use of simple models and a lack of knowledge about possible local equilibrium between the defect populations. We therefore present in Table 1 the values proposed most recently in [64,70,71]. The results provide evidence for a divacancy which is more mobile than the monovacancy and a divacancy binding energy in the range ∿0.1 - 0.2 eV. We note that it is difficult to derive a binding energy from the free energy of binding listed in Table 1, since both the sign and magnitude of the binding entropy are unknown[70].

2.2.4 copper

Great difficulties have been encountered in obtaining reproducible results with quenched Cu since it dissolves both of the gaseous impurities O and H. The annealing spectra which have been obtained[72-77] after quenching under a variety of conditions show considerable differences as shown in Fig. 7a. Also, the temperature range over which the annealing of mobile defects has been observed is more spread out than in the previous cases of Au, Al and Pt. These results have led to considerable disagreement in the literature regarding the mobilities of the vacancy defects.

All investigators find a first annealing stage near 275 K (see first group of encircled points in Fig. 7a). The relative importance of this stage varies considerably in different experiments from very small[75] to large[75,77]. It is also well established that many of the mobile defects anneal to large clusters which in turn anneal out at considerably higher temperatures (second group of encircled points in Fig. 7a). There is disagreement, however, about the presence or absence of additional intermediate annealing stages in the intermediate region between the

encircled data in Fig. 7a. The presence or absence of these stages apparently depends upon the experimental procedure and the "cleanliness" of the quenching technique. As noted in the caption to Fig. 7a, Cu has been quenched under both reducing atmospheres (CO and H_2) and under what were undoubtedly oxidizing atmospheres ($\sim N_2$, $\sim Ar$). Furthermore, the quenching medium has usually been water which can itself be a source of contamination as shown by Wright and Evans[76]. These investigators demonstrated that H can be picked up from a water quenching bath maintained at room temperature. Furthermore, they found it necessary to boil the water to expel dissolved gases and to use specially cleaned containing vessels in order to obtain reproducible results.

Convincing evidence has been given[74,76,77] that the highest purity quenches are achieved when a reducing atmosphere containing CO is employed. None of the intermediate peaks shown in Fig. 7a appeared when CO was used except for one small one reported in [76]. Also, Wright and Evans[76] and Bourassa and Lengeler[77] found that the resistivity increments quenched into Cu in a CO atmosphere are reproducible and are also consistent with expected vacancy defect concentrations. Widely scattered and inconsistent results had often been obtained with other atmospheres in the earlier work (see discussion in [78]). We therefore conclude that none of the intermediate stages in Fig. 7a are well established and that most (and quite possibly all) are associated with impurities, most notably O.

The only intrinsic defect annealing stage which has been established experimentally is therefore the one occurring near 280 K (encircled in Fig. 7a). The migration energy for this stage has been measured to be 0.74 eV[77] and 0.71 eV[76] in specimens quenched in CO atmospheres. Following Bourassa and Lengeler[77], we therefore assign monovacancy annealing to this stage and take 0.72 eV as the monovacancy migration energy (Table 1). This value will be found to be consistent with annealing data after irradiation and reasonably consistent with monovacancy formation energy and self-diffusion data. It is interesting to note that there is no evidence for the presence of highly mobile divacancies in this stage, since only one

constant activation energy if found.

2.2.5 silver

Silver dissolves the gaseous impurities O and H, and, as in the previous case of Cu, great difficulties have been encountered in achieving reproducible quenching results. The annealing spectra obtained in a number of studies[74,79-83] are shown in Fig. 8a, and it is seen that the results show considerable disagreement and are spread over a relatively wide temperature range in a manner quite similar to that of Cu. The high temperature annealing stages near 600 K are undoubtedly associated with the annealing out of relatively immobile clusters. Several, but not all, investigators find a first annealing stage near 260 K (see group of encircled points in Fig. 8a), and there is lack of agreement about the presence, or absence, of annealing stages due to mobile defects at the intermediate temperatures. As noted in the caption to Fig. 8a, widely different quenching techniques were employed, and considerable differences existed in the degrees of "cleanliness" achieved by the different investigators. An examination of the experiments shows that the first low temperature stage encircled in Fig. 8a was observed only in specimens quenched under what appear to be particularly clean conditions. This stage was observed by Doyoma and Koehler[81] (who used an ultra pure He gas quenching atmosphere enclosed in a gettered and cryo-pumped capsule), Cuddy and Machlin[82] (who also used an ultra pure He gas quench) and Clarebrough, et al.[74] (who used a reducing CO atmosphere in order to eliminate O). It is also seen that little further annealing occurred in these "clean" experiments until considerably higher temperatures ($\gtrsim$550 K) were reached. On the other hand, the low temperature stage near 260 K is missing, and additional stages are found at intermediate temperatures near 340 and 450 K in the experiments of Quéré[79,83] and Ramsteiner, et al.[80] where less pure quenching atmospheres of Ar or N_2 were used. Therefore, these latter stages can evidently be associated with impurity effects.

We conclude that the only intrinsic stage due to mobile defects which has been clearly resolved in Ag is the first stage near 260 K. The effective migration energy in this stage has been measured to be 0.57 eV in both [81] and [82]. This energy is too low for monovacancy migration (see below), and following Doyoma and Koehler and Cuddy and Machlin we tentatively assign it to divacancy migration (Table 1). The picture of the annealing spectrum which emerges therefore is one in which divacancies control the annealing directly after quenching. Upon warming, appreciable clustering occurs until at considerably higher temperatures ($\gtrsim$550 K) the clusters begin to anneal. At no point is there any clear evidence for annealing controlled by monovacancy migration.

2.2.6 tungsten

It is only recently that reasonably successful quenching experiments have been accomplished with W. The BCC metals are especially susceptible to contamination by interstitial impurities, and the removal of these impurities and the attainment of clean quenching conditions has been a long standing difficulty (see various papers in [4] and [6]). These problems have been dealt with by using electron-beam zone melted specimens of high purity[84-89] and a quenching technique which involves either a quench into a bath of superfluid He or rapid radiation cooling in vacuo. The mobile defects anneal out in one main stage located in the range 850 to 1170 K [84,86,89] as indicated in Fig. 9a[†]. No fine structure has been detected in the individual annealing peaks, and, as usual, the peak temperature tends to decrease as the defect concentration (quenching temperature) increases.

For some time the question of whether the resistivity increments quenched into W have really been due to vacancy defects and not impurities has been in doubt. Kunz[85] provided the first evidence in favor of vacancies by demonstrating that Stage I

[†] We neglect here a smaller higher temperature stage observed in [86]. The temperature of this stage is nearly independent of temperature and is probably associated with some form of impurity-induced clustering.

in irradiated W is enhanced in previously quenched specimens. In this case the quenched-in vacancies evidently provide extra annihilation sites for the interstitials which migrate in Stage I. In further work Park, et al.[88] have studied the defects quenched into W directly by field ion microscopy and have found $\sim 2 \times 10^{-5}$ atomic fraction of atomic "dark spot" defects in a specimen quenched from 3300 K. These dark spot defects were presumably due to either vacancy defects or impurity atoms. However, the observed defect contrast was identical to that expected of vacancy defects, and additional work[90,91] has shown that the concentration of these dark spots exceeded the concentration of contrast-producing impurity atoms expected on the basis of detailed chemical analyses of the specimens. Furthermore, this defect concentration is not inconsistent with the concentration of vacancies expected on the basis of the magnitudes of the resistivity increments quenched into W and current estimates of the resistivity of the vacancies. These field ion microscopy results therefore seem consistent with the presence of quenched-in vacancies. However, experiments with additional specimens in the same laboratory showed that the quenched-in resistivity increment[88,90,91], and also the concentration of observed dark spot defects[90] decreased with an increased number of electron beam melting zone passes used in the original specimen preparation. This result is disturbing, since it suggests that fewer defects were quenched in as the specimen was increasingly purified by increasing the number of zone passes. However, no evidence was found for such purification by means of chemical analysis[91]. It is therefore possible that the electron beam melting introduced some type of impurity at a very small concentration which nucleated vacancy precipitation and therefore caused losses during quenching.† Recently, Rasch, Siegel and Schultz[89] have found small voids in quenched and subsequently annealed W by electron microscopy. The observed void distributions were not inconsistent with those expected on the basis of the clustering of quenched-in vacancies. Of particular interest was the

† An investigation of this possibility by electron microscopy is currently underway[92].

observation of denuded zones at grain boundaries which is typical of vacancy defect behavior in quenched specimens. Most recently, Metz, et al.[93] have studied positron annihilation in W at elevated temperatures under equilibrium conditions and have obtained results which indicate the presence of vacancies at concentration levels consistent with the above results.

In view of all of these results we may assume that the resistivity increments quenched into W are indeed due to vacancies. Unfortunately, there is appreciable scatter in the quenched-in resistivity data obtained in different investigations[84-91]. As pointed out above, and also in [89], it appears likely that trace impurities in W are often capable of nucleating vacancy precipitation during quenching, and that small differences in these concentrations may therefore strongly affect the number of vacancies retained. Also, different fixed sink densities are undoubtedly present in different specimens and this would also tend to produce a scatter in the results. Efforts[88,90,91] to correct for such losses by extrapolating the quenched-in resistivity increments to infinite quenching rates have not served to eliminate the observed differences. However, it is possible that this could be the case for certain loss mechanisms particularly if the nucleation and growth of vacancy precipitates at relatively high temperatures is involved.

In view of this situation there is a difficulty in deriving a monovacancy formation energy from the temperature dependence of the measured quenched-in resistivity increments. Somewhat surprisingly, there is fair agreement for the effective vacancy defect formation energy if the results of the different investigators are examined. Gripshover, et al.[84] report a value E^f_{eff}=3.6 eV while the Stuttgart group[89] obtains 3.9 eV. If the Cornell results[88,90,91] for specimens with small numbers of zone passes and large quenched-in increments are employed, an average result of 3.7 eV is found. An overall average of 3.7 eV is therefore obtained which is not greatly different from the value E^f_{lv}~3.5 eV determined in [93] from positron annihilation experiments. We therefore take E^f_{lv} ~ 3.6 eV as the best current estimate for the monovacancy formation energy (Table 3). The latest and probably most reliable, annealing

experiments after quenching are those in [89] in which an effective migration energy of 1.8 eV was determined (Table 1). Taking $E^f_{1v} \sim 3.6$ eV we find that the value $E^m_{1v} = 1.8$ is not inconsistent with $E^m_{1v} + E^f_{1v} = Q_{1v}$ when $Q_{1v} < 5.7$ as determined recently by Mundy[94] (Table 3). Insufficient data are available to allow us to draw any conclusions about divacancy properties.

2.2.7 molybdenum

The problem of attaining high purity in quenching experiments with Mo has been even more severe than in W, and discussions of many of the difficulties may be found in [4,6]. The most recent and also cleanest quenching and annealing experiments seem to be those of Suezawa and Kimura[95] who found an annealing stage at $T_a = 628$ K after a quench from 2330 K (Fig. 10a). Even in this work evidence of a progressive buildup of some type of contamination during annealing after quenching was found. Measurements of the effective migration energy in this stage[95] showed wide scatter leading to the value $E^m_{eff} \sim 1.6 \pm 0.3$ eV. A value of $E^f_{eff} \sim 3.2$ eV was also arrived at after rough corrections were made for the loss of vacancy defects to sinks during quenching. Therefore, $E^m_{eff} + E^f_{eff} \sim 4.8$ eV in apparent agreement with $Q \sim 4.$ to 4.9 eV[96,97] (see Table 3). We therefore take $\sim 1.6 \pm 0.3$ eV as the best estimate of E^m_{1v} currently available from quenching experiments (Table 1).

2.3 Discussion of Quenching Results

The above results clearly indicate the great difficulties which may be caused by impurities in quenching experiments. The most complete results have been obtained with the three FCC metals least susceptible to impurity effects, i.e., Au, Al and Pt, while the least satisfactory situation seems to exist for the BCC metal Mo. The results also indicate that reasonably reliable information about the nature of the vacancy defect species which anneal out in quenched specimens can only be obtained when extensive annealing data obtained from well controlled experiments are available and where computer modeling techniques are used to construct self-consistent models of the entire quenching and subsequent annealing process.

In order to carry out such a program it is essential to have extensive auxiliary information such as equilibrium defect concentration data and self-diffusion data. The work with Au also indicates the need for a knowledge of the structure and properties of the sinks in the quenched and annealed specimens. Unfortunately, efforts along these lines have only been made so far with Au and Al.

The results in Table 1 for the FCC metals indicate that divacancies are generally more mobile than divacancies in these metals and possess binding energies which are probably in the range 0.1-0.3 eV. The rather extensive results obtained for Au and Al both suggest that trivacancies are at least as mobile as divacancies in FCC lattices and are not particularly strongly bound, i.e., $E^b_{3v} \sim 1.5\ E^b_{2v}$. Furthermore, these defects appear to play a significant role in the annealing kinetics over rather a wide range of conditions. The results for the BCC metals are generally less satisfactory. It now seems quite well established that vacancies are indeed quenched into at least the BCC metals W and Mo. However, the quenching and annealing data are not sufficiently precise or extensive to allow the determination of highly accurate monovacancy migration and formation energies. Nevertheless, values are obtained which are not inconsistent with available self-diffusion data. No significant information about divacancy properties in the BCC metals can be obtained at present because of the rather limited nature of the data. (We remark that divacancy behavior in the BCC lattice is probably quite different than in the FCC lattice, since a nearest-neighbor divacancy in the BCC lattice cannot migrate easily as a nearest-neighbor pair[98].

3. ANNEALING OF VACANCY DEFECTS IN IRRADIATED SPECIMENS

3.1 Introductory Comments

During irradiation equal numbers of vacant and interstitial sites are produced. If a specimen is irradiated at very low temperatures and then warmed, these defects become mobile in different temperature ranges and, as is well known, anneal out progressively in a series of more or less distinct annealing stages. The problem

of extracting information about vacancy defect properties from annealing experiments in these stages is complicated by the fact that the vacancy defects and their anti-defects, the interstitial defects, are usually present simultaneously and that essentially all of the annealing occurs by mutual annihilation. This situation injects an element of symmetry into the problem which makes it difficult to determine experimentally which type of defect is the mobile one in a given annealing process. The problem of the identification of the type of defect which migrates in each annealing stage has been exhaustively reviewed recently in [2-7] and, therefore, we shall not attempt a detailed discussion of the situation. Suffice it to say that two major (and differing) interpretations of the experimental facts have emerged, i.e., the "one interstitial model" and the "two interstitial model".

The major features of the annealing spectrum of Cu in terms of the one interstitial model are shown in Fig. 11. The first defects to execute long range migration are highly mobile interstitials which migrate in Stage I where they may annihilate frozen-in vacancies or form interstitial or interstitial-impurity clusters.† During Stage II coarsening of the interstitial type clusters occurs along with some further annihilation of frozen-in vacancies. Finally, the vacancies become mobile in Stage III where they may annihilate interstitials at the interstitial clusters, form vacancy clusters or annihilate at fixed sinks. In Stage IV various rearrangements and coarsening processes occur until finally in Stage V the vacancy clusters are able to dissociate thermally and all excess defects are eliminated by self-diffusion processes. Variations in this scheme occur for different metals. In Au the interstitial is apparently unusually mobile, and long range interstitial migration therefore occurs at an exceedingly low temperature. In Al and Pt very few interstitial and vacancy clusters survive Stage III, and recovery is essentially complete at the end of this stage.

In the two interstitial model it is assumed that two types of interstitials can

† A very small fraction of the interstitials may also reach fixed sinks, of course (see Appendix A.18).

be produced, i.e., a metastable interstitial and a stable interstitial which can be produced by conversion of the metastable interstitial to the stable form. The metastable interstitial is highly mobile and executes long range migration in Stage I. The stable interstitial is considerably less mobile and only becomes mobile at a higher temperature which is either below or almost coincident with the temperature at which vacancies become mobile. In this model Stage III is then associated with the migration of the stable interstitial and a further stage (Stage IV) is associated with vacancy defect migration. Stage III is generally lower than Stage IV (e.g., Pt) but may be almost coincident in certain cases (e.g., Al). This model has enormous flexibility due to its many parameters and has been introduced in order to take account of certain experimental observations which have been reported over the years (see [2-7] for details).

After years of experimentation and discussion it now seems (at least to the present writer!) that there is sufficient evidence available to indicate that the one interstitial model is basically correct for FCC and BCC metals and therefore that vacancy defect migration takes place in Stage III. The body of evidence is described briefly in the Appendix. The various items listed there differ considerably in their persuasiveness and in some cases are merely circumstantial. Certain of the experiments can also be interpreted in terms of the two interstitial model but they often require more complex (and hence more unlikely) explanations. The Appendix must therefore be considered collectively as a body of information which favors vacancy defect migration in Stage III. In the remainder of the present review we therefore proceed on the basis of the one interstitial model.

The detailed nature of Stage III annealing has been extensively discussed by Schilling and coworkers[15,99,100], and we shall therefore mention only a few important points. As already pointed out, Stage III involves the long range migration of vacancy defects to either interstitial clusters which are already present due to the prior aggregation of highly mobile interstitials or to vacancy type clusters which build up during the annealing by vacancy defect aggregation. The resulting

kinetics are usually close to second order, and T_a is therefore shifted to lower temperatures as the initial concentration of defects is increased. For the irradiation doses which are commonly employed the sink structure which is produced is relatively dense, and the average number of jumps taken by the migrating vacancy defects is therefore relatively small in comparison to the situation in quenching experiments where the migrating vacancy defects anneal out on a coarser scale to vacancy aggregates or fixed sinks. Under these conditions it might be expected that the interactions between the migrating vacancy defects would be less extensive in Stage III annealing than in quenched specimens and, on average, effects due to the formation and migration of mobile clusters such as divacancies might be reduced. It was originally hoped, therefore, that annealing under typical Stage III conditions would be mainly due to monovacancies and therefore be particularly simple, particularly after electron irradiation[15]. However, it has been found, for example in Pt[99], that divacancy contributions can be important under certain conditions and that complex kinetics can exist.

3.2 Results of Irradiation Experiments

The Stage III annealing temperature, T_a, found for the different metals are shown in Figs. 1b, 5b-10b. These temperatures correspond to the maxima of the isochronal annealing peaks found by various investigators as in the case of the quenching data discussed previously. Results for irradiations with electrons, neutrons and other fast particles are included, and no attempt has been made to discriminate between results obtained with different particles, dose levels, irradiation temperatures or isochronal heating rates. Two closely spaced Stage III isochronal annealing peaks often appear when displacement cascade damage is produced because of the presence of both correlated and uncorrelated vacancy defect annealing in such cases[15]. In these instances we have taken T_a as the temperature of the uncorrelated annealing peak which appears at the higher temperature. We note that in general, no clearcut fine structure was detectible in any of the observed

peaks. Examination of Figs. 1b, 5b-10b shows that the Stage III annealing temperatures are generally spread over an appreciable range of temperature for each metal as might be expected in view of the different defect concentrations and sink structures which were undoubtedly present in the different experiments. Also included in Figs. 1b, 7b, 8b, 10b are the temperatures found for the onset of vacancy defect migration in the damage rate experiments of Antesberger, et al.[108] (see Appendix section A.16). These temperatures fall well within the observed Stage III temperature ranges.

In a number of cases migration energies have been measured in Stage III, and the results are summarized in Table. 2.

For Au, Al and Cu apparently constant migration energies were found in the Stage III region. In the case of Ag Gordon[147] found values ranging over the rather wide range 0.71-0.57 eV with an average value given by 0.64 eV. For Pt several investigators found apparently constant values, but very detailed and extensive measurements in [66] revealed a systematic variation of E^m_{eff} which was interpreted in terms of a mono-divacancy model with $E^m_{1v} = 1.45$, $E^m_{2v} = 1.00$ and $E^b_{2v} = 0.15$ eV. These latter results are particularly important, since they indicate that Stage III annealing can be complex. For W and Mo values of $\sim$1.7 and $\sim$1.3 eV respectively have been found.

4. DISCUSSION

Comparison of the average Stage III annealing temperatures in Figs. 1b, 5b-10b with the corresponding average annealing temperatures for the mobile defects obtained by quenching (Figs. 1a, 5a-10a) shows that the Stage III temperatures are generally lower. This result may be attributed to the fact that, on average, the number of defect jumps to annihilation is considerably smaller in the irradiation experiments than in the quenching experiments because of a greater effective sink density in the former experiments. This may be demonstrated in a rough way by plotting the average annealing temperature, $\overline{T}_a$ versus the effective migration energy E^m_{eff} for

both types of experiments as in Fig. 12. As shown now such a plot should be approximately linear and intersect the origin whenever the annealing processes in the various metals are closely the same with respect to initial defect concentration, form of the kinetics, heating rate, sink density, etc. Under many conditions the annealing rate may be represented to a good approximation by a relationship of the form

$$\frac{dc}{dt} = A(T) \cdot f(c) \cdot \exp(- E^m_{eff}/kT). \qquad (1)$$

The factor $A(T)$ depends upon the sink geometry, the frequency factor for defect migration and other factors which may be mildly temperature dependent. If the specimen is heated at a constant rate, α, i.e.,

$$T = \alpha t \quad , \qquad (2)$$

we may integrate eq. (1) in the form

$$\int_{c_o}^{c} \frac{dc}{f(c)} = F(c,c_o) = \frac{1}{\alpha} \int_{o}^{T} A(T) \cdot \exp(-E^m_{eff}/kT)\, dT \qquad (3)$$

where c_o = initial defect concentration. Since $A(T)$ is only mildly temperature dependent, the temperature dependence of the integral on the right hand side of eq. (3) is dominated by the temperature dependence of $\exp(-E^m_{eff}/kT)$, and if c_o, the form of the kinetics, etc. remain the same for the different metals as mentioned above, the integrated result may be written, to a reasonably good approximation in the form

$$c \simeq c(X) \quad , \qquad (4)$$

where,

$$X \equiv \frac{E^m_{eff}}{kT} \, . \qquad (5)$$

Therefore, the maximum annealing rate during isochronal annealing (which occurs at the temperature T_a) corresponds to a fixed value of X (i.e., X = constant = E^m_{eff}/kT_a), and a linear relationship between E^m_{eff} and T_a is predicted for the different metals. The averaged irradiation results fall remarkably well on a single curve, whereas the averaged quenching results fall reasonably well on a second curve corresponding

to higher $\overline{T}_a$ values. In constructing the curve for annealing after irradiation values of E^m_{eff} from Table 3 and average values of T_a for Figs. 1b, 5b-10b were used. For the curve for annealing after quenching E^m_{eff} = 0.71 eV was used for Au (Section 2.2.3). Average values of T_a were obtained from Figs. 1a, 5a-10a. As explained below, we believe that the best value for E^m_{lv} for Mo is 1.3 eV (Table 3). Therefore, E^m_{eff} for Mo after quenching is probably near the low end of the range indicated in Fig. 12. The true deviation for Mo from the curve which is drawn is therefore probably small.

The difference between the two curves can be well explained if the average number of defect jumps to annihilation during annealing after quenching is $\sim 10^3$ larger than after irradiation. The result that the number of jumps after quenching is generally larger than after irradiation has been well noted by others in the literature. Detailed considerations of this point may be found elsewhere[15,37, 66,112,164].

Of further interest in this respect are experiments in which specimens are first quenched and then irradiated at low temperatures and finally annealed through Stage III. The phenomena which occur in such experiments have been discussed by Schilling, et al.[15]. An unquenched specimen (electron irradiated) shows the usual single main Stage III annealing peak. However, after quenching and irradiation two peaks generally appear, one at a temperature slightly below that of the original Stage III peak in the unirradiated specimen and a second peak well above the temperature of the original Stage III peak. The first peak represents the usual Stage III annealing of vacancy defects to interstitial and vacancy clusters. However, the higher concentration of vacancy defects introduced by the quench shifts this peak to a temperature somewhat below the usual Stage III temperature. The second peak represents the annealing of the remaining vacancy defects in the absence of the interstitial sinks (which have already been removed in the lower temperature annealing stage). These vacancy defects anneal out in a manner similar to that in a quenched specimen at a temperature which is above the normal

Stage III annealing temperature because of the relatively low density of sinks available for the vacancy defect annealing. The results of such experiments are fully consistent with our present conclusions. A computer simulation of such kinetics has been given by Johnson[164].

The average values of E^m_{eff} observed after irradiation obtained from Table 2 are listed in Table 3 and may be compared there with the values of E^m_{1v} derived from the quenching and annealing experiments. Rather satisfactory agreement is obtained in general and in view of our limited present state of knowledge regarding the details of Stage III annealing we tentatively associate these activation energies with monovacancy annealing. We note that this assignment indicates that E^m_{1v} for Ag is about 0.66 eV which is significantly larger than the divacancy migration energy E^m_{2v} = 0.57 eV obtained from the quenching experiments (Table 1) as should be the case.

"Best values" of E^m_{1v} are next obtained in Table 3 (column 4) by combining the results of the irradiation and quenching experiments. For the FCC metals we merely average the results. However, for the BCC metals we weight the results towards the irradiation values, since in our opinion the latter values are more reliable (see Sections 2.2.6 and 2.2.7).

"Best values" of the monovacancy formation energy, E^f_{1v}, are also listed in Table 3. These were obtained by averaging the results obtained from positron annihilation measurements (column 5) with results obtained from measurements of the dependence of the quenched-in resistivity on T_q in quenching experiments (column 6). Finally, the sum [E^m_{1v} (best) + E^f_{1v} (best)] is compared with the activation energy for self-diffusion due to monovacancies, Q_{1v} in the last two columns of Table 3. The values of Q_{1v} were derived in most cases from self-diffusion data taken at relatively low temperatures in order to avoid possible divacancy contributions. It is seen that reasonably good agreement is obtained and that apparently self-consistent values of E^m_{1v} and E^f_{1v} now exist for most of these metals. This important result provides strong support for the viewpoints adopted in the present work.

An interesting aspect of the above results is the fact that reasonable self-consistency is attained between values of E_{1v}^m determined near Stage III temperatures and values of E_{1v}^f and Q_{1v} determined at higher temperatures in the range of self-diffusion temperatures. This result indicates that the temperature dependence of E_{1v}^m must be relatively small as is predicted by the estimates made in [174].

We conclude by emphasizing that our knowledge of the properties of small clusters (including divacancies) is extremely limited. As may be seen in Table 1 only a few values of divacancy migration energies and binding energies have been listed for FCC metals. We remark that the value of E_{2v}^b for Au most likely lies much nearer 0.25 than 0.57 eV. Also, it is noted that the value $E_{2v}^b = 0.15$ obtained for Pt from annealing experiments after irradiation (Table 2) is in rough agreement with values obtained in quenching experiments (Table 1). Values of E^m and E^b for higher order clusters are almost non-existent although a start at determining these quantities has been made with Au and Al. No attempt has been made in the present review to discuss migrational and binding entropies, since the state of our knowledge of these parameters is even more limited than that for migrational and binding energies.

In view of the difficulties mentioned at the beginning of this paper it appears that further progress will depend upon the development of further techniques sensitive to the behavior of particular defects and the performance of further well controlled and characterized experiments supported by computer modeling studies.

ACKNOWLEDGMENTS

The writer wishes to express his thanks to a number of colleagues who provided valuable assistance in the preparation of this review. These include A. Bourret, J. S. Koehler, B. Lengeler, N. L. Peterson, R. P. Sahu, H. Schultz, D. N. Seidman, R. W. Siegel, K. Sonnenberg and particularly W. Schilling. The work was supported by the Energy Research and Development Administration under Contract E(11-1)-2679. Additional support was received from the National Science Foundation through the Materials Science Center at Cornell University.

APPENDIX. EVIDENCE FOR VACANCY DEFECT ANNEALING IN STAGE III AFTER IRRADIATION

In the following we list various observations which on an overall basis favor the one-interstitial model and the migration of vacancy defects in Stage III.

A.1) The great majority of current theoretical calculations predict highly mobile interstitials which should migrate in Stage I. Johnson[175] concludes that if high energy interstitial migration in Stage III is accepted then it must be concluded that present calculations are inadequate to describe defect properties.

A.2) The effective defect migration energies derived from Stage III annealing experiments correlate reasonably well with the monovacancy migration energies obtained from quenching experiments (see Table 3).

A.3) The sum of the migration energy obtained from Stage III annealing measurements and the monovacancy formation energy agrees reasonably well with the activation energy for self-diffusion due to monovacancies (see Table 3).

A.4) There is no convincing evidence that an additional Stage IV exists which is due to a second elementary defect which becomes mobile just above Stage III. According to the two-interstitial model such a stage is required in many metals in order to accommodate the stable interstitial in Stage III and the monovacancy in Stage IV. We believe that annealing stages found in this regime have often been due to impurity effects as, for example, in quenched Cu (Fig. 7) and quenched Ag (Fig. 8).

A.5) An extensive series of x-ray diffuse scattering and electron microscopy experiments[100] indicates that in all pure metals studied so far <u>there are relatively few single interstitials left by the time Stage III</u> is reached. Instead, they have undergone long range migration in or above Stage I (depending upon irradiation temperature and thermal history) and have formed aggregates (usually dislocation

loops). Furthermore, above Stage III the density of interstitial clusters is strongly reduced. Since the clusters are too tightly bound to dissociate thermally at Stage III temperatures the results must be due to the long range migration of vacancy defects to the loops causing annihilation.

A.6) Schilling, et al.[100] have shown that for an irradiated metal containing point defects the ratio formed by dividing the "Stokes-Wilson" diffuse x-ray scattering by the relative change in lattice parameter is independent of the total defect density but is sensitive to the state of agglomeration of the interstitials and vacancies. They then cite measurements of this ratio for Cu which indicate that essentially all of the interstitials become clustered below Stage III and that vacancy migration and clustering occur in Stage III.

A.7) At very small scattering angles x-ray scattering from defect structures becomes sensitive mainly to changes in local electron density. Measurements by Haubold[176] on electron irradiated copper warmed through Stage III show a relatively large corresponding increase in low angle x-ray scattering. This result appears to be consistent with the migration and clustering of vacancies in Stage III, since estimated scattering effects due to changes in the state of the interstitial clustering should be much smaller.

A.8) So far, no clearcut annealing stage due to long range interstitial migration has been found at low temperatures in Au[177]. It has been argued[178] that the apparent absence of such direct evidence for the long range migration of a mobile interstitial in Stage I is due to the fact that metastable interstitials introduced by low temperature migration immediately convert to stable interstitials which migrate freely only when the specimen is warmed through Stage III. However, x-ray diffuse scattering measurements[177] show that no significant concentrations of single interstitials are present in Au electron irradiated at 5 K. Instead, they are mainly present in small interstitial clusters. Furthermore, on annealing in Stage II the cluster size increases. These results appear to preclude the long range

migration of any free interstitials in Stage III.

A.9) In a number of metals observed in the electron microscope changes in the defect structure caused by annealing through Stage III have been found which may be interpreted on the basis of long range vacancy migration. Shimomura[179] observed interstitial clusters in electron irradiated Au below Stage III in the electron microscope. Upon warming through Stage III the interstitial clusters shrank and disappeared presumably as a result of the migration of vacancy defects to the clusters. Shimomura also carried out similar experiments with silver[180] and obtained basically the same results. In other work Bourret[181] found interstitial clusters in irradiated Al below Stage III and found that these nearly all annealed out during warming through Stage III presumably as a result of the migration of vacancy type defects.

A.10) Thin gold foils containing vacancy type precipitates have been bombarded on one face with low energy ions[182]. Under these conditions interstititals were injected below the surface while any vacancies were left behind essentially at the incident surface. Electron microscope observation revealed that the sizes of the vacancy precipitates were reduced by the irradiation at large distances, i.e., $\gtrsim$1000 Å, from the incident surface at temperatures as low as 25 K, i.e., well below Stage III. These results were taken as an indication that the injected interstitials were mobile throughout the entire temperature range studied and that after injection they migrated from positions relatively near the incident surface to the vacancy clusters causing annihilation. On the other hand Seeger[183] has claimed that the results can be explained by the propagation of very long replacement collision sequences (RCS's) in gold having ranges of the order of 2000 Å. In such a case the vacancy precipitates are eliminated directly by the injected RCS's, no low temperature interstitial mobility is required, and it is then possible for interstitials to become mobile in Stage III as in the two interstitial model. However, the existence of such long range RCS's seems doubtful. Ecker [184] has made direct measurements of the transmission of RCS's through Au

foils and concludes that the range must be <50 Å. More recently, Ayrault and Seidman [185] have carried out further direct transmission measurements and have concluded that the range must be far less than 2000 Å†. Finally, other evidence reviewed recently by Blewett, et al.[186] is also in disagreement with a range as large as 2000 Å.

A.11) Attardo and Galligan[187] have examined neutron irradiated W in the field ion microscope and have reported the apparent annealing of "bright spot" defects and vacancy defects near Stage III. Jeannotte and Galligan[188] have observed the annealing of vacancy defects in neutron irradiated W near Stage III-IV temperatures in the field ion microscope. The bright spots in [187] were elongated along <110>, and the work in [187] and [188] has been interpreted as evidence for a Stage III <110> split interstitial and vacancy migration in Stage IV. However, this work has been reviewed recently by Seidman, et al.[189] who argue that these experiments are inconclusive. Initially impure W was used in [188], and in both [187] and [188] relatively large concentrations of Re were produced by transmutation. Seidman, et al.[189] conclude that the bright spot defects observed in [187] were probably interstitial-Re atom complexes. Seidman has also pointed out elsewhere[190] that the evidence published by Attardo, et al.[187] for the existence of a <110> split interstitial in W must be regarded with caution, since the atom-by-atom dissection of high index planes in the field ion microscope is required before any conclusions can be reached about the geometric configuration of an interstitial defect. The same cautionary statement applies to the claim of Attardo and Galligan[191] that Stage III in neutron irradiated Pt is caused by the migration of a <100> split interstitial.

A.12) Seidman, et al.[189] have made an extensive search with the field ion microscope for a converted Stage III interstitial in high purity electron and ion irradiated W. No evidence was found for the existence of such a defect.

---

† We note that this most recent result is in disagreement with the earlier preliminary results reported in the review of Blewitt, et al. [186].

A.13) Vogel and Mansel[192] have irradiated Al containing a dilute concentration of Co at a temperature between Stages I and III where the interstitials are mobile and become trapped at the Co atoms. The trapping is detected by the appearance of a new isomer-shifted line in the Mössbauer spectrum. During subsequent Stage III annealing the resistivity and the new Mössbauer line anneal out in parallel fashion. Here, the resistivity monitors the removal of vacancy-trapped interstitial pairs, whereas the new Mössbauer line monitors only the removal of the trapped interstitials. The conceivable detrapping of interstitials from the Co atoms can be ruled out as an explanation by a consideration of the form of the observed kinetics. Also, the conceivable diffusion of the Co atom-interstitial complexes to the vacancies can be ruled out by the absence of any Co clustering. Therefore, it must be concluded that vacancies migrate to the trapped interstitials and cause annihilation.

A.14) Positron annihilation measurements on irradiated Mo[155,193,194] and Cu[195-197] warmed through Stage III show effects which can be explained most readily by the migration of vacancies and the formation of small vacancy clusters in this stage.

A.15) A series of Cu specimens has been doped with Frenkel pairs at 4 K and then annealed to a series of increasing temperatures, T_d, above Stage I and then cooled back to 4 K[198]. When T_d is below Stage III the defects in each of these doped specimens consist of single vacancies and interstitial clusters. However, when T_d is above Stage III the doping defects consist of vacancy and interstitial clusters. A test dose of defects is then introduced at 4 K, the specimen is warmed to a fixed annealing temperature between Stage I and Stage III, and is again cooled to 4 K. The fraction, r_I, of the test defects remaining after the warming to above Stage I is then measured. A sharp increase in r_I is found when T_d passes through Stage III. This must be due to the migration

and clustering of the doping vacancy defects in Stage III. The clustering of these defects causes them to be much less efficient in capturing the test interstitials which become mobile at temperatures above Stage I, thereby producing the observed increase in r_I.

A.16) Antesberger, et al.[108] have "doped" Cu, Ag, Au and Mo specimens with a distribution of interstitial and vacancy clusters by an irradiation and annealing procedure. They then introduced "test defects" by electron irradiation and measured the damage rate as a function of irradiation temperature. The density of doping defects was large enough, and the density of test defects was small enough, so that any test defects escaping correlated recombination in Stage I interacted almost exclusively with the doping defects. As the irradiation temperature was increased, a large drop-off in the damage rate occurred in Stage I when the interstitials became mobile and began to annihilate at correlated vacancies and the doping defects. A long flat plateau followed as the annihilation of the interstititals became independent of temperature and the damage rate became constant. When Stage III was reached the damage rate decreased sharply again and either went essentially to zero (for Au and Mo) or else exhibited another plateau at a much reduced value (Cu and Ag). The large observed decrease in the damage rate in Stage III and the behavior at higher temperatures is highly consistent with the onset of vacancy migration in Stage III. The almost zero damage rate above Stage III in Cu and Ag may have been due to differences in the configurations of the doping defects in these metals or other small impurity effects since the Au was apparently more pure initially than either the Cu or Ag. It is interesting to note that no increases in the damage rate were observed anywhere which may have been due to the conversion of Stage I interstitials to "Stage III interstitials" as postulated in the two-interstitial model[178].

A.17) Damage rate measurements in Stage II have been made by Becker, et al.[199] for Cu during electron irradiation at 93 K. Evidence is found that isolated immobile

interstitials are not produced under these conditions. Instead mobile interstitials are produced, and the resulting damage consists of immobile vacancies and interstitial clusters which are nucleated at impurity atoms and grow by the aggregation of the mobile interstitials. Upon subsequent annealing of such a structure an annealing stage is found in the Stage III temperature range which is very similar to that normally found after electron irradiation at 4 K. Since vacancies are the only isolated defects present in such a structure, these results indicate vacancy defect annealing in Stage III.

A.18) Gruber et al.[200] have made parallel measurements of the recovery of the lattice parameter and the resistivity of irradiated Cu after low temperature irradiation. By analyzing these measurement they find a small excess concentration of vacancies (relative to interstitials) in Stage I and a small excess concentration of interstitials (relative to vacancies) in Stage III. This is just the result to be expected if interstitials migrate in Stage I and vacancies migrate in Stage III. The long range migration of either type of defect results in a small preferential loss of that defect at fixed sinks thereby producing a corresponding small excess concentrati n of the anti-defect.

A.19) Kornelsen[201] has irradiated W specimens with 5 keV heavy ions at room temperature, annealed the damaged specimens to T_A, injected the specimens with 250 eV He ions at room temperature, and then studied the thermal desorption spectra of the helium atoms during subsequent warming to temperatures as high as 2400 K. He finds a strong desorption peak at ∿1560 K which is largely eliminated by the preliminary annealing of the damaged specimens to temperatures near T_A = 700 K. Kornelsen explains this result in the following manner. Single injected helium atoms are mobile in W at room temperature and are strongly trapped at any monovacancies present in the ion damaged specimens. Helium atoms trapped in this manner are subsequently detrapped (desorbed) by heating to ∿1560 K. The elimination of this trapping-detrapping process by the preliminary annealing of the damaged specimens to T_A ∿ 700 K

is due to the fact that the monovacancy traps are removed by such an anneal, i.e., vacancy migration occurs in Stage III near 700 K. In later work by Caspers, et al.[202] similar experiments have been performed with Mo, and it has again been concluded that vacancies migrate in Stage III. In this work additional experiments were performed which demonstrated that in at least Mo the vacancy annealing in Stage III was due to the migration of vacancies and not to the migration of interstitials to immobile vacancies.

A.20) Federighi, et al.[51] have pointed out that the defects which are mobile in Stage III of Al interact in the same manner with certain impurity elements as do vacancies under well understood conditions. Furthermore, the defects which are mobile in Stage III produce the same clustering of Zn atoms in Al as vacancies do, whereas the defects moving at lower temperatures do not produce any clustering. These results suggest that the defects mobile in Stage III are indeed vacancies.

A.21) Kiritani[203] has reviewed studies of the nucleation and growth of point defect clusters in a variety of metals (e.g., Cu, Au, Al, Pt, Mo, W) during electron irradiation in a high voltage microscope over a wide temperature range (10-1000 K). Analysis of the variation of the nucleation rate of interstitial clusters and the growth behavior of interstitial dislocation loops leads to results which are consistent with interstitial migration in Stage I and vacancy migration in Stage III.

REFERENCES

1. R. M. J. Cotterill, M. Doyoma, J. J. Jackson and M. Meshii (eds.), Lattice Defects in Quenched Metals (Academic Press, New York, 1965).

2. A. Seeger, D. Schumacher, W. Schilling and J. Diehl (eds.), Vacancies and Interstitials in Metals (North-Holland, Amsterdam, 1970).

3. Preprint of Conference Papers, International Conference on Vacancies and Interstitials in Metals, Berichte der Kernforschungsanlage Jülich - Jül - Conf - 2 (Vols. 1 and 2) Jülich GmbH, Jülich, W. Germany (1968).

4. R. deBatist, J. Nihoul and L. Stals (eds.), Defects in Refractory Metals (Studiecentrum voor Kernenergie, Mol, 1972).

5. R. Bullough (ed.), J. Phys. F. 3, No.2 (1973).

6. R. J. Arsenault (ed.), Nucl. Metall. 18 (1973) 1-608.

7. M. T. Robinson and F. W. Young, Jr. (eds.), Fundamental Aspects of Radiation Damage in Metals (National Technical Information Service, Springfield, VA, 22161 (USA) 1975).

8. A. Seeger and D. Schumacher, ref. [1], p. 15.

9. R. W. Balluffi and R. W. Siegel, ref. [1], p. 693.

10. J. W. Kauffman and G. J. Dienes, Acta Met. 13 (1965) 1049.

11. K. P. Chik, D. Schumacher and A. Seeger, in Phase Stability in Metals and Alloys, P. S. Rudman (ed.), (McGraw-Hill, New York, 1967) p. 449.

12. R. A. Johnson, Phys. Rev. 174 (1968) 684.

13. K. P. Chik, ref. [2], p. 183.

14. R. W. Balluffi, K. H. Lie, D. N. Seidman and R. W. Siegel, ref. [2], p. 125.

15. W. Schilling, G. Burger, K. Isebeck and H. Wenzl, ref. [2], p. 255.

16. N. H. March and J. S. Rousseau, Cryst. Latt. Defects 2 (1971) 1.

17. R. W. Balluffi, ref. [7], p. 852.

18. J. J. Burton and D. Lazarus, Phys. Rev. B 2 (1970) 787.

19. K. C. Jain and R. W. Siegel, to be published.

20. R. P. Sahu and R. W. Siegel, to be published.

21. R. P. Sahu, K. C. Jain and R. W. Siegel, to be published.

22. K. C. Jain and R. W. Siegel, Phil. Mag. 25 (1972) 105.

23. F. Cattaneo, E. Germagnoli and G. Guarini, Supplemento al Nuovo Cimento 1 (1963) 282.

24. T. Kino and J. S. Koehler, Phys. Rev. 162 (1967) 632.

25. C. G. Wang, D. N. Seidman and R. W. Balluffi, Phys. Rev. 169 (1968) 553.

26. M. deJong and J. S. Koehler, Phys. Rev. 129 (1963) 40.

27. M. deJong and J. S. Koehler, Phys. Rev. 129 (1963) 49.

28. R. W. Balluffi and D. N. Seidman in Radiation-Induced Voids in Metals, J. W. Corbett and L. C. Ianniello (eds.) (CONF-710601, National Technical Information Service, U.S. Dept. of Commerce, Springfield, VA 22151, 1972) p. 563.

29. J. E. Bauerle and J. S. Koehler, Phys. Rev. 107 (1957) 1493.

30. W. Schüle, A. Seeger, D. Schumacher and K. King, Phys. Stat. Sol. 2 (1962) 1199.

31. R. M. J. Cotterill, J. Phys. Soc. Japan 18, Supple. III (1963) 48.

32. R. L. Segall and L. M. Clarebrough, Phil. Mag. 9 (1964) 865.

33. D. Schumacher, Phys. Letters 19 (1965) 367.

34. J. Bass, Phys. Rev. 137 (1965) A765.

35. J. deLaplace, J. Hillairet, C. Mairy and Y. Adda, Mem. Sci. Rev. Met. 63 (1966) 282.

36. H. I. Dawson and K. B. Das, ref. [3], p. 125.

37. C. Lee and J. S. Koehler, Phys. Rev. 176 (1968) 813.

38. A. Camanzi, N. A. Mancini, E. Rimini and E. Schianchi, ref. [3], p. 154.

39. K. Nakata, K. Ikeuchi, H. Hirano, K. Furukawa and J. Takamura, ref. [7], p. 622.

40. R. M. J. Cotterill, Phil. Mag. 6 (1961) 1351.

41. J. A. Ytterhus and R. W. Balluffi, Phil. Mag. 11 (1965) 707.

42. R. W. Siegel, Phil. Mag. 13 (1966) 337.

43. J. W. Kauffman and M. Meshii, ref. [1], p. 77; M. Meshii and J. W. Kauffman, Acta Met. 8 (1960) 815.

44. D. G. Franklin and H. K. Birnbaum, Acta Met. 19 (1971) 965.

45. A. S. Nowick and B. S. Berry, Anelastic Relaxation in Crystalline Solids (Academic Press, New York, 1972) p. 304.

46. R. K. Sharma, C. Lee and J. S. Koehler, Phys. Rev. Lett. 19 (1967) 1379.

47. C. Panseri and T. Federighi, Phil. Mag. 3 (1958) 1223.

48. M. Doyoma and J. S. Koehler, Phys. Rev. 134 (1964) A522.

49. T. Federighi, ref. [1], p. 217.

50. C. Budin and P. Lucasson, Phys. Lett. 16 (1965) 229.

51. T. Federighi, S. Ceresara and F. Pieragostini, Phil. Mag. 12 (1965) 1093.

52. C. Budin and P. Lucasson in Interaction of Radiation with Solids, A. Bishay (ed.) (Plenum, New York, 1967) p. 497.

53. J. Hillairet, V. Levy and G. Revel, C. R. Acad. Sci. Paris 271 (1970) 1228.

54. R. Brugiere and P. Lucasson, Mem. Sci. Rev. Met. 69 (1972) 277.

55. B. Roebuck and K. M. Entwistle, Phil. Mag. 25 (1972) 153.

56. V. Levy, J. M. Lanore and J. Hillairet, Phil. Mag. 28 (1973) 373.

57. P. Tzanetakis, J. Hillairet and G. Revel, Phys. Stat. Sol. (b) 75 (1976) 433.

58. V. Levy, J. M. Lanore and J. Hillairet, Phil. Mag. 28 (1973) 389.

59. W. DeSorbo and D. Turnbull, Phys. Rev. 115 (1959) 560.

60. M. Kiritani, H. Murakami, A. Yoshinaka, A. Sato and S. Yoshida, J. Phys. Soc. Japan 29 (1970) 1494.

61. J. J. Jackson, ref. [1], p. 467.

62. J. J. Jackson, ref. [1], p. 479.

63. J. Polak, Phys. Stat. Sol. 21 (1967) 581.

64. D. Schumacher, A. Seeger and O. Härlin, Phys. Stat. Sol. 25 (1968) 359.

65. R. Rattke, O. Hauser and J. Wieting, Phys. Stat. Sol. 31 (1969) 167.

66. K. Sonnenberg, W. Schilling, K. Mika and K. Dettmann, Rad. Eff. 16 (1972) 65.

67. A. Ascoli, M. Asdente, E. Germagnoli and A. Manara, J. Phys. Chem. Sol. 6 (1958) 59.

68. G. L. Bacchella, E. Germagnoli and S. Granata, J. Appl. Phys. 30 (1959) 748.

69. G. R. Piercy, Phil. Mag. 5 (1960) 201.

70. A. S. Berger, D. N. Seidman and R. W. Balluffi, Acta. Met. 21 (1973) 123, 137.

71. J. Polak, Phys. Lett. 24A (1967) 649.

72. D. G. Martin, Phil. Mag. 7 (1962 803.

73. A. Lucasson, P. Lucasson and C. Budin, J. Phys. 25 (1964) 1004.

74. L. M. Clarebrough, R. L. Segall, M. H. Loretto and M. E. Hargreaves, Phil. Mag. 9 (1964) 377.

75. F. Ramsteiner, G. Lampert, A. Seeger and W. Schüle, Phys. Stat. Sol. 8 (1965) 863.

76. P. Wright and J. H. Evans, Phil. Mag. 13 (1966) 521.

77. R. R. Bourassa and B. Lengeler, J. Phys. F. 6 (1976) 1405.

78. R. O. Simmons and R. W. Balluffi, Phys. Rev. 129 (1963) 1533.

79. Y. Quéré, C. R. Acad. Sci. 252 (1961) 2399.

80. F. Ramsteiner, W. Schüle and A. Seeger, Phys. Stat. Sol. 2 (1962) 1005.

81. M. Doyoma and J. S. Koehler, Phys. Rev. 127 (1962) 21.

82. L. J. Cuddy and E. S. Machlin, Phil. Mag. 7 (1962) 745.

83. Y. Quéré, J. Phys. Soc. Japan 18, Supple. III (1963) 91.

84. R. J. Gripshover, M. Khoshnevisan, J. S. Zetts and J. Bass, Phil. Mag. 22 (1970) 757.

85. W. Kunz, Phys. Stat. Sol. (b) 48 (1971) 387.

86. W. Kunz and H. Schultz, ref. [4], p. 99.

87. H. Schultz, ref. [6], p. 394.

88. J. Y. Park, H-C. W. Huang, A. S. Berger and R. W. Balluffi, ref. [6], p. 420.

89. K.-D. Rasch, R. W. Siegel and H. Schultz, to be published.

90. J. Y. Park, Ph.D. Thesis, Cornell University (1975).

91. H-C. W. Huang, Ph.D. Thesis, Cornell University (1975).

92. J. Y. Park, R. W. Siegel and R. W. Balluffi, research in progress.

93. H. Metz, H. Stoll, W. Trost, K. Maier, H.-E. Schaefer and D. Herlach, this Conference.

94. J. N. Mundy (private communication).

95. M. Suezawa and H. Kimura, Phil. Mag. 28 (1973) 901.

96. J. Askill and D. H. Tomlin, Phil. Mag. 8 (1963) 997.

97. L. V. Pavlinov and V. N. Bykov, Fiz. Metall. Metalloved. 18 (1964) 145.

98. H. Mehrer, P. Kunz and A. Seeger, ref. [4], p. 183.

99. W. Schilling and K. Sonnenberg, ref. [5], p. 322.

100. W. Schilling, P. Ehrhart and K. Sonnenberg, ref. [7], p. 470.

101. W. Schilling, G. Burger, K. Isebeck and H. Wenzl, ref. [2], Fig. 50, p. 329.

102. W. Bauer and A. Sosin, Phys. Rev. 136 (1964) A474.

103. F. Dworschak, K. Herschbach and J. S. Koehler, Phys. Rev. 133 (1964) A293.

104. K. Wittmaack, Phys. Stat. Sol. 37 (1970) 633.

105. W. Bauer, Phys. Lett. 19 (1965) 180.

106. S. Okuda, S. Takamura and H. Maeta, ref. [3], p. 317.

107. K. Herschbach and J. J. Jackson, Phys. Rev. 153 (1967) 694.

108. G. Antesberger, H. Schroeder, K. Sonnenberg and U. Dedek, ref. [7], p. 575.

109. C. Dimitrov-Frois and O. Dimitrov, ref. [3], p. 290.

110. A. Sosin and L. H. Rachal, Phys. Rev. 130 (1963) 2238.

111. K. Isebeck, R. Müller, W. Schilling and H. Wenzl, Phys. Stat. Sol. 18 (1966) 467.

112. Y. N. Lwin, M. Doyoma and J. S. Koehler, Phys. Rev. 165 (1968) 787.

113. S. Ceresara, T. Federighi and D. Gelli, Nuovo Cimento 29 (1963) 1244.

114. W. Schilling, G. Berger, K. Isebeck and H. Wenzl, ref. [2], Fig. 40, p. 320.

115. K. R. Garr and A. Sosin, Phys. Rev. 162 (1967) 681.

116. R. Brugiere and P. Lucasson, Phys. Stat. Sol. 24 (1967) K77.

117. P. B. Peters and P. E. Shearin, Phys. Rev. 174 (1968) 691.

118. K. Herschbach and J. J. Jackson, Phys. Rev. 177 (1969) 1049.

119. M. Doyoma, J. S. Koehler, Y. N. Lwin, E. A. Ryan and D. G. Shaw, Phys. Rev. B3 (1971) 1069.

120. N. Kontoleon K. Papathanassopoulos and K. Chountas, Rad. Eff. 20 (1973) 273.

121. C. Dimitrov, ref [7], p. 608.

122. G. Berger, K. Isebeck, J. Völkl, W. Schilling and H. Wenzl, Z. Angew. Phys. 22 (1967) 452.

123. W. Schilling, G. Berger, K. Isebeck and H. Wenzl, ref. [2], Fig. 49, p. 329.

124. W. Bauer, Rad. Eff. 1 (1969) 23.

125. U. Himmler, H. Peisl, A. Sepp and W. Waidelich, ref. [3], p. 343.

126. W. Schilling and K. Sonnenberg, ref. [5], Fig. 13, p. 337.

127. W. Schilling, G. Berger, K. Isebeck and H. Wenzl, ref. [2], Fig. 57, p. 344.

128. G. Duesing and W. Schilling, Rad. Eff. 1 (1969) 65.

129. W. Bauer and A. Sosin, Phys. Rev. 147 (1966) 482.

130. J. J. Jackson and K. Herschbach, Phys. Rev. 164 (1967) 951.

131. M. Doyoma, J. S. Koehler, Y. N. Lwin, E. A. Ryan and D. G. Shaw, Phys. Rev. B4 (1971) 281.

132. W. Schilling, G. Berger, K. Isebeck and H. Wenzl, ref. [2], Fig. 39, p. 320.

133. W. Schilling, G. Berger, K. Isebeck and H. Wenzl, ref. [2], Fig. 56, p. 341.

134. W. Schilling, G. Berger, K. Isebeck and H. Wenzl, ref. [2], Fig. 54, p. 337.

135. F. Dworschak and J. S. Koehler, Phys. Rev. 140 (1965) A941.

136. W. Bauer and A. Sosin, Phys. Lett. 24A (1967) 193.

137. R. Brugiere and P. Lucasson, Phys. Stat. Sol. 30 (1968) K139.

138. W. Schilling and K. Sonnenberg, ref. [5], Fig. 15, p. 340.

139. G. Antesberger, K. Sonnenberg, P. Weinhold, R. R. Coltman, C. E. Klabunde, J. M. Williams and R. L. Chaplin, ref. [7], p. 561.

140. J. W. Corbett, R. B. Smith and R. M. Walker, Phys. Rev. 114 (1959) 1460.

141. C. J. Meechan and J. A. Brinkman, Phys. Rev. 103 (1956) 1193.

142. C. P. Cannon and A. Sosin, Rad. Eff. 25 (1975) 253.

143. G. Roth and V. Naundorf, ref. [3], p. 364.

144. C. J. Meechan, A. Sosin and J. A. Brinkman, Phys. Rev. 120 (1960) 411.

145. P. Weinhold, Thesis TH Aachen.

146. C. Budin, P. Lucasson and A. Lucasson, J. Phys. 26 (1965) 9.

147. A. Gordon, Ph.D. Thesis, University of Illinois, 1969.

148. L. K. Keys and J. Moteff, J. Appl. Phys. 40 (1969) 3866.

149. L. K. Keys and J. Moteff, J. Nucl. Mats. 34 (1970) 260.

150. H. H. Neely, D. W. Keefer and A. Sosin, Phys. Stat. Sol. 28 (1968) 675.

151. G. H. Kinchin and M. W. Thompson, J. Nucl. Energy 6 (1958) 275.

152. M. W. Thompson, Phil. Mag. 5 (1960) 278.

153. H. B. Afman, J. H. Mooy and H. Rademaker, Scripta Met. 4 (1970) 545.

154. W. Schilling (private communication).

155. J. H. Evans and M. Eldrup, Nature 254 (1975) 685.

156. H. B. Afman, Phys. Stat. Sol. (a) 13 (1972) 623.

157. G. Goedemé, B. M. Pande, L. Stals and J. Nihoul, Rad. Eff. 3 (1970) 275.

158. L. K. Keys, J. P. Smith and J. Moteff, Phys. Rev. Lett. 22 (1969) 57.

159. L. Stals, J. Nihoul, J. Cornelis and P. DeMeester, Phys. Stat. Sol. (a) 18 (1973) 283.

160. L. Stals, ref. [4], p. 91.

161. P. Moser, ref. [4], p. 88.

162. H. E. Kissinger, J. L. Brimball and E. P. Simonen, ref. [7], p. 568.

163. L. K. Keys and J. Moteff, J. Appl. Phys. 41 (1970) 2618.

164. R. A. Johnson, Phys. Rev. B1 (1970) 3956.

165. W. Triftshäuser and J. D. McGervey, Appl. Phys. 6 (1975) 177.

166. R. Jank and W. Triftshäuser, to be published.

167. B. Lengeler, Phil. Mag. 34 (1976) 259.

168. A. Seeger and H. Mehrer, Phys. Stat. Sol. 29 (1968) 231.

169. C. Y. Sun, Ph.D. Thesis, University of Illinois (1971).

170. A. Seeger and H. Mehrer, ref. [2], p. 1.

171. C. V. Kidson and R. Ross, Proceedings International Conference on Radioisotopes in Science Research, Paris, 1 (1957) p. 185: F. Cattaneo and E. Germagnoli, Phil. Mag. 7 (1962) 1373.

172. H. Mehrer and A. Seeger, Phys. Stat. Sol. 35 (1969) 313: K. Maier, C. Bassani and W. Schüle, Phys. Lett. A44 (1973) 539: M. Weithase and F. Noack, Z. Phys. 270 (1974) 319.

173. J. G. E. M. Backus, H. Bakker and H. Mehrer, Phys. Stat. Sol. (b) 64 (1974) 151: N. Q. Lam, S. J. Rothman, H. Mehrer and L. J. Nowicki, Phys. Stat. Sol. (b) 57 (1973) 225.

174. L. M. Levinson and F. R. N. Nabarro, Acta Met. 15 (1967) 785: A. S. Nowick and G. J. Dienes, Phys. Stat. Sol. 24 (1967) 461: L. A. Girifalco, Scripta Met. 1 (1967) 5: C. P. Flynn, Phys. Rev. 171 (1968) 682.

175. R. A. Johnson, ref. [5], p. 295.

176. H.-G. Haubold, ref. [7], p. 268.

177. P. Ehrhart and E. Segura, ref. [7], p. 295.

178. A. Seeger, ref. [7], p. 493.

179. Y. Shimomura, Phil. Mag. 19 (1969) 773.

180. Y. Shimomura, J. Appl. Phys. 41 (1970) 749.

181. A. Bourret, in Electron Microscopy and Structure of Materials, G. Thomas (ed.) (University of California Press, 1972) p. 974.

182. G. J. Thomas and J. A. Venables, Phil. Mag. 28 (1973) 1171.

183. A. Seeger, Rad. Eff. 2 (1970) 165.

184. K. H. Ecker, Rad. Eff. 23 (1974) 171.

185. G. Ayrault and D. N. Seidman, private communication (1976).

186. T. H. Blewitt, M. A. Kirk and T. L. Scott, ref. [7], p. 152.

187. M. J. Attardo, J. M. Galligan and J. G. Y. Chow, Phys. Rev. Lett. 19 (1967) 73.

188. D. Jeannotte and M. J. Galligan, Acta Met. 18 (1970) 71.

189. D. N. Seidman, K. L. Wilson and C. H. Nielsen, ref. [7], p. 373.

190. D. N. Seidman, ref. [5], p. 393.

191. M. J. Attardo and J. M. Galligan, Phys. Rev. Lett. 17 (1966) 1173.

192. G. Vogl and W. Mansel, ref. [7], p. 349.

193. M. Eldrup and O. E. Mogensen, ref. [7], p. 1127.

194. M. Eldrup, O. E. Mogensen and J. H. Evans, J. Phys. F. 6 (1976) 499.

195. S. Mantl and W. Triftshäuser, Phys. Rev. Lett. 34 (1975) 1554.

196. S. Mantl and W. Triftshäuser, ref. [7], p. 1122.

197. J. G. Byrne, P. Alexopoulas, F. Alex, T. D. Hadnagy, R. Waki, G. R. Miller and R. W. Ure, 4th Int. Conf. on Positron Annihilation, Helsingor, Denmark, (August, 1976) p. 59.

198. G. Antesberger, K. Sonnenberg, P. Weinhold, R. R. Coltman, C. E. Klabunde and J. M. Williams, ref. [7], p. 657.

199. D. E. Becker, F. Dworschak and H. J. Wollenberger, Phys. Stat. Sol. (b) 17 (1971) 171.

200. E. E. Gruber, J. A. Tesk, T. H. Blewitt and R. E. Black, Phys. Rev. B2 (1970) 2849.

201. E. V. Kornelsen, Rad. Eff. 13 (1972) 227.

202. L. M. Caspers, A. van Veen, A. A. van Gorkum, A. v.d. Beukel and C. M. van Baal, to be published.

203. M. Kiritani, ref. [7], p. 695.

Table 1. Selected values of vacancy defect migration energies and binding energies obtained from quenching experiments (eV).

Metal	E^m_{1v}	E^m_{2v}	E^m_{3v}	E^b_{2v}	E^b_{3v}	Ref.
Au	0.83-0.89	0.62-0.79	0.48-0.56	0.25-0.57	1.5 E^b_{2v}	[21]
Al	0.65	0.50	0.47	0.20	∿0.3	[58]
Pt	1.45	1.10	----	0.19	----	[71]
	1.38	1.11	----	0.11	----	[64]
	----	----	----	0.23†	----	[70]
Cu	0.72	----	----	----	----	[76,77]
Ag	----	0.57	----	----	----	[81,82]
W	1.8	----	----	----	----	[89]
Mo	1.3 - 1.9	----	----	----	----	[95]

† This is the value of the free energy of binding at T = 443 K.

Table 2. Effective migration energies for Stage III annealing after irradiation (eV).

Metal	Irrad.	E^m_{eff}	Ref.
Au	electrons	0.80	[102]
	protons	0.80	[103]
	electrons	0.85	[37]
	gold ions	0.77	[104]
Al	neutrons	0.59	[109]
	neutrons	0.58	[111]
	electrons	0.61	[115]
	electrons	0.58	[116]
	electrons	0.58	[124]
	neutrons	0.59	[113]
	electrons	0.62	[112]
	electrons	0.58	[52]
	neutrons	0.61	[120]
Pt	neutrons	1.46	[69]
	electrons	1.36	[129]
	electrons	1.45	[131]
	electrons	1.45 = E^m_{1v} 1.00 = E^m_{2v} 0.15 = E^b_{2v}	[66]
Cu	electrons	0.67	[144]
	protons	0.71	[135]
	protons	0.71	[103]
	electrons	0.69	[137]
	neutrons	0.72	[134]
	electrons	0.71	[139]
	electrons	0.71	[145]
Ag	protons	0.67	[103]
	electrons	0.64 (avg.)	[147]
W	neutrons	1.66	[149]
		1.7	[151]
		1.7	[152]
Mo	electrons	1.29	[153]
	electrons	1.29	[156]
	neutrons	1.29	[160]

Table 3. "Best values" of E^m_{1v}, E^f_{1v} and Q_{1v} (eV).

Metal	E^m_{1v} (quench) from Table 1	E^m_{eff} (irrad) from Table 2	E^m_{1v} (best value)	E^f_{1v} (positron)	E^f_{1v} (quench)	E^f_{1v} (best value)	E^m_{1v} (best) + E^f_{1v} (best)	Q_{1v} (best value)
Au	0.83-0.89	0.81	0.83	0.97 [165]	0.94 [21,167]	0.95	1.78	1.76 [168]
Al	0.65	0.59	0.62	0.66 [166]	0.69 [57]	0.67	1.29	1.28 [169,170]
Pt	1.42	1.43	1.43	----	1.51 [61]	1.51	2.94	2.9 [171]
Cu	0.72	0.70	0.71	1.29 [155]	1.27 [77]	1.28	1.98	2.07 [172]
Ag	----	0.66	0.66	1.16 [155]	1.10 [81,82]	1.13	1.79	1.76 [173]
W	1.8	1.69	1.7	∿3.5 [93]	∿3.7 [89]	∿3.6	∿5.3	<5.7 [94]
Mo	1.3 - 1.9	1.29	1.3	----	∿3.2 [95]	∿3.2	∿4.5	∿4.5 [96,97]

FIGURE CAPTIONS

Figure 1: (a) Display of annealing temperatures, T_a, corresponding to the maxima of the isochronal annealing peaks observed for Au after quenching[27,29-40]. Filled circles connected by tie-lines correspond to cases where substructure consisting of two, or more, closely spaced maxima was found in the same specimen. Encircled points at high temperatures correspond to the annealing of large vacancy clusters.
(b) Same as (a) except for irradiated Au[37,39,101-107]. Data point X corresponds to vacancy defect annealing temperature obtained from damage rate measurements[108].

Figure 2: (a) Annealing temperature, T_a, versus quenching temperature, T_q, for quenched Au[29-39].
(b) Same as (a) except for quenched Al[47-57].

Figure 3: (a) Annealing peak for quenched Au which exhibits substructure [36].
(b) - (d) Annealing spectra for quenched Al[56].

Figure 4: Effective migration energy, E^m_{eff}, versus vacancy defect concentration in quenched Au. Cross-hatched band contains data obtained by a number of other investigators[25,35,41-43].

Figure 5: (a) Display of annealing temperatures, T_a, corresponding to the maxima of the isochronal annealing peaks observed for Al after quenching[47-57]. Filled circles connected by tie-lines correspond to cases where two closely spaced maxima were found in the same specium. Encircled points at high temperatures correspond to the annealing of large vacancy clusters.
(b) Same as (a) except for irradiated Al[51,52,54,109-125].

Figure 6: (a) Display of annealing temperatures, T_a, corresponding to the maxima of the isochronal annealing peaks observed for Pt after quenching[61-66].
(b) Same as (a) except for irradiated Pt[66,69,107,126-131].

Figure 7: (a) Display of annealing temperatures, T_a, corresponding to the maxima of the isochronal annealing peaks observed for Cu after quenching. Points connected by tie-lines correspond to cases where successive annealing stages were found in the same specimen. Encircled group of points at the higher temperatures corresponds to the annealing of large vacancy clusters. ○ quenched into methyl alcohol under vacuum[72]; ● quenched in H_2 or He[73]; ▩ quenched into H_2O under Ar by "Method 1"[75]; △ quenched into H_2O under N_2 + H_2[75]; ▲ quenched into H_2O under Ar or Ar + ethyl

alcohol[75]; ▽ quenched into H_2O under CO[74]; ▼ quenched into H_2O under Ar[74]; ▷ quenched into H_2O under CO + N_2[76]; ▶ quenched into H_2O under N_2[76]; □ quenched into HCl under CO + He[77].
(b) Same as (a) except for irradiated Cu[103,106,122,125,132-146]. Data point X corresponds to vacancy defect annealing temperature obtained from damage rate measurements[108].

Figure 8: (a) Display of annealing temperatures, T_a, corresponding to the maxima of the isochronal annealing peaks observed for Ag after quenching. Points connected by tie-lines correspond to cases where successive annealing stages were found in the same specimen. ◁ , ◀ quenched in N_2 or Ar[79]; ▽ , ▼ , ▷ , ▶ quenched into H_2O under Ar + air[80]; ▲ quenched in He[81]; ○ quenched in He[82]; ● , □ quenched in N_2 gas or liquid nitrogen[83]; ■ quenched into H_2O under Ar[74]; △ quenched into H_2O under CO[74].
(b) Same as (a) except for irradiated Ag[103,122,147]. Data point X corresponds to vacancy defect annealing temperature obtained from damage rate measurements[108].

Figure 9: (a) Display of annealing temperatures, T_a, corresponding to the maxima of the isochronal annealing peaks observed for W after quenching[84,86,89].
(b) Same as (a) except for irradiated W[85,148-150].

Figure 10: (a) Display of annealing temperature, T_a, corresponding to the maximum f the isochronal annealing peak observed in Mo after quenching[95].
(b) Same as (a) except for irradiated Mo[148,153-163]. Data point X corresponds to vacancy defect annealing temperature obtained from damage rate measurements[108].

Figure 11: Schematic diagram of the annealing stage spectrum of Cu according to the one-interstitial model for defect annealing after low temperature irradiation.

Figure 12: Effective migration energy, E^m_{eff}, versus average annealing temperature, $\overline{T}_a$, for annealing after irradiation and after quenching (see text for details).

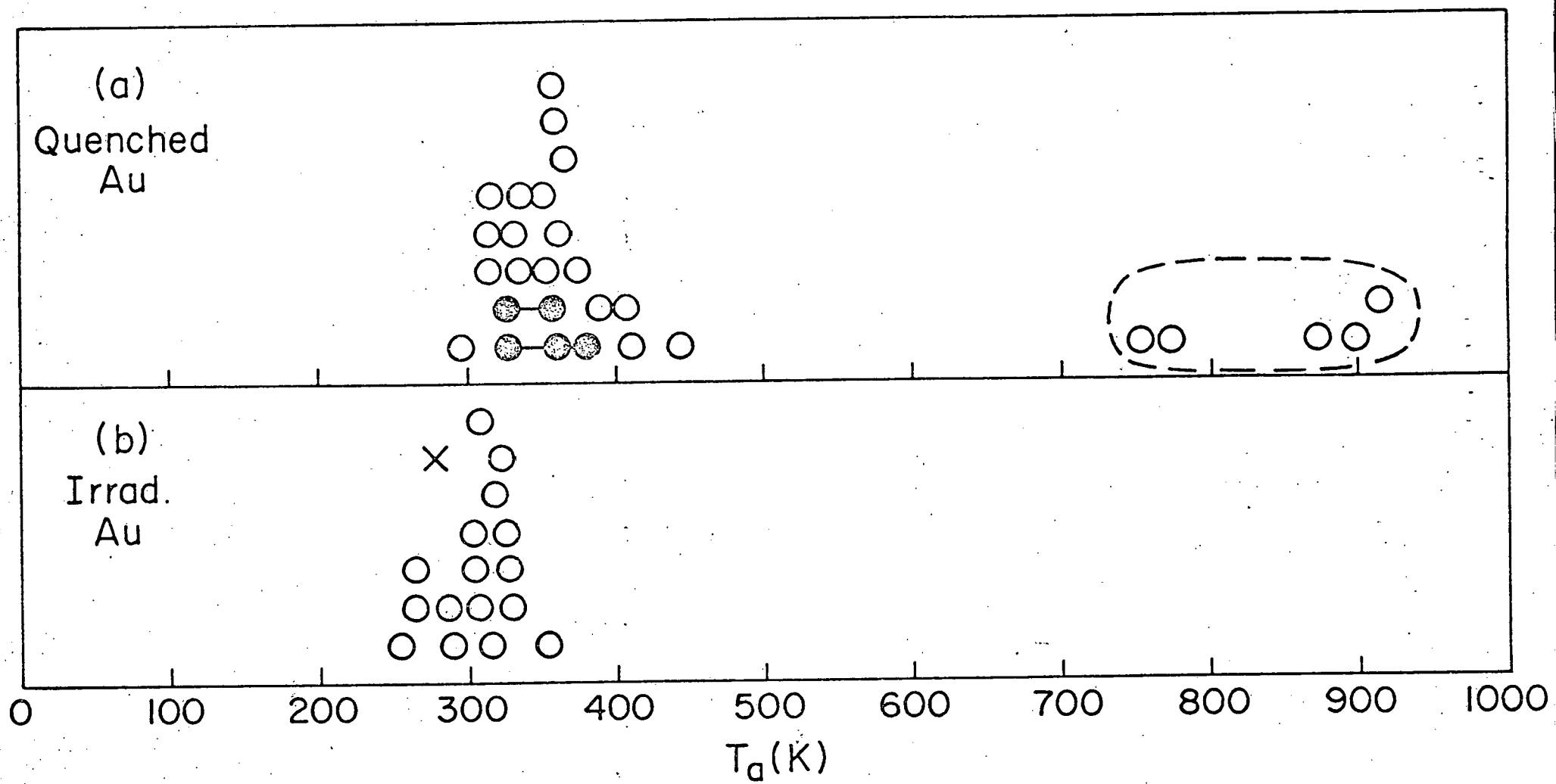
(a)
Quenched
Au
(b)
Irrad.
Au
0
100
200
300
400
500
600
700
800
900
1000
T_a(K)

FIG 1

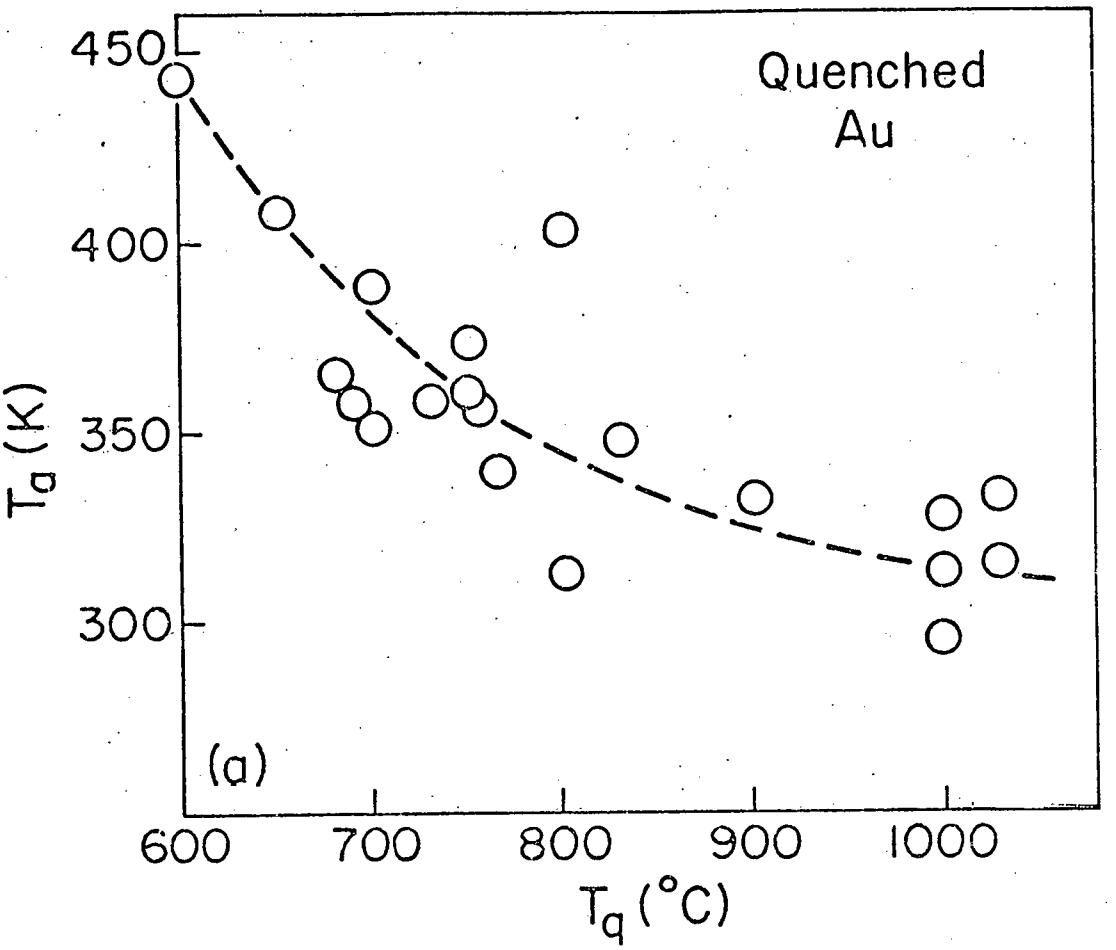
Quenched
Au
450
400
350
300
T_a (K)
(a)
600
700
800
900
1000
T_q (°C)

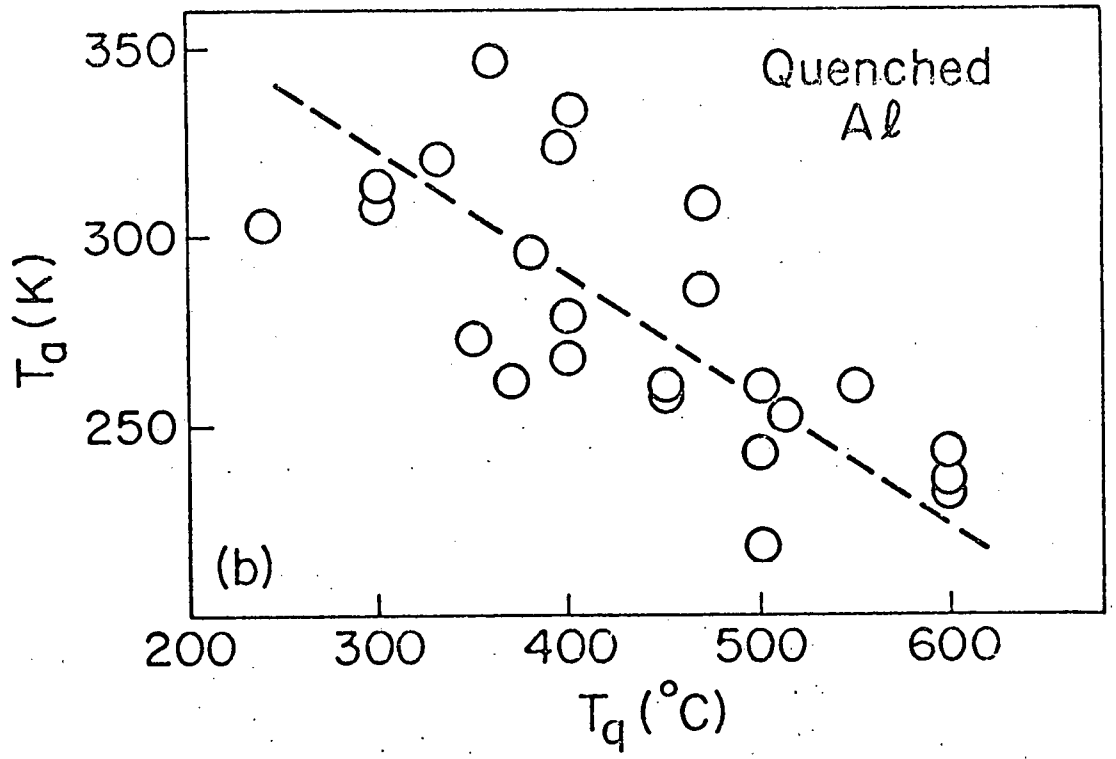
Quenched
Al
350
300
250
T_a (K)
(b)
200
300
400
500
600
T_q (°C)

FIG 2

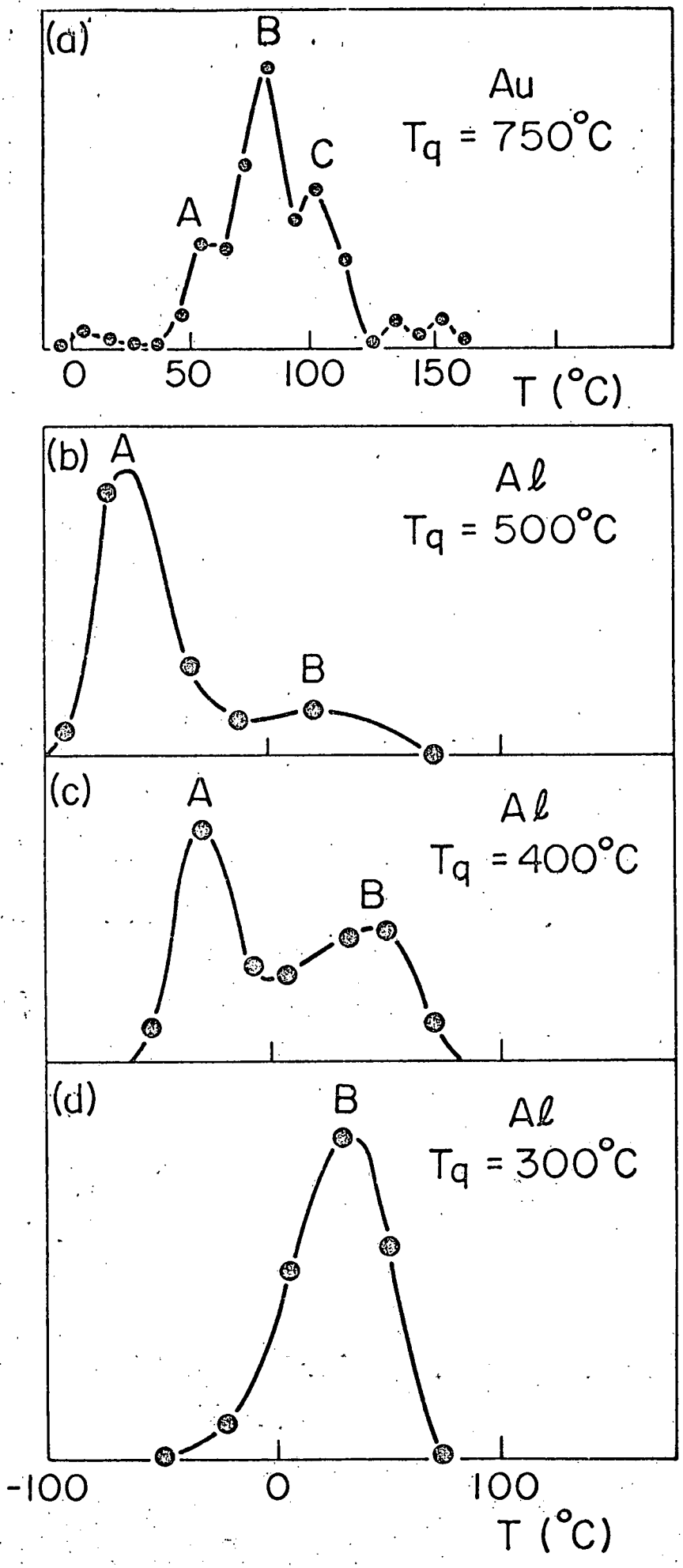
(a)
B
Au
T_q = 750°C
C
A
0
50
100
150
T (°C)
(b) A
Aℓ
T_q = 500°C
B
(c)
A
Aℓ
T_q = 400°C
B
(d)
B
Aℓ
T_q = 300°C
-100
0
100
T (°C)

FIG 3

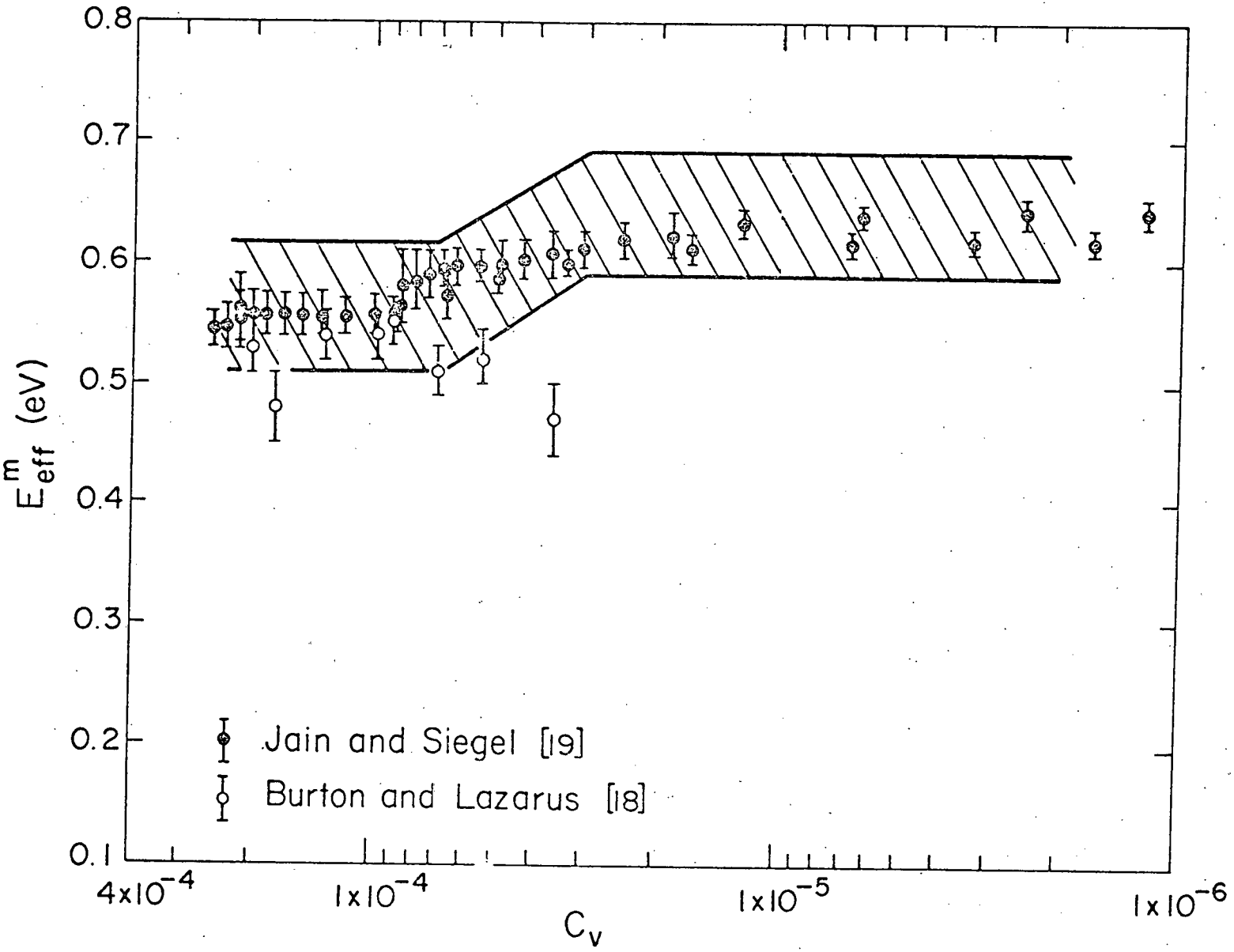
0.8
0.7
0.6
0.5
0.4
0.3
0.2
0.1
E^m_{eff} (eV)
Jain and Siegel [19]
Burton and Lazarus [18]
4×10^{-4}
1×10^{-4}
1×10^{-5}
1×10^{-6}
C_v

FIG 4

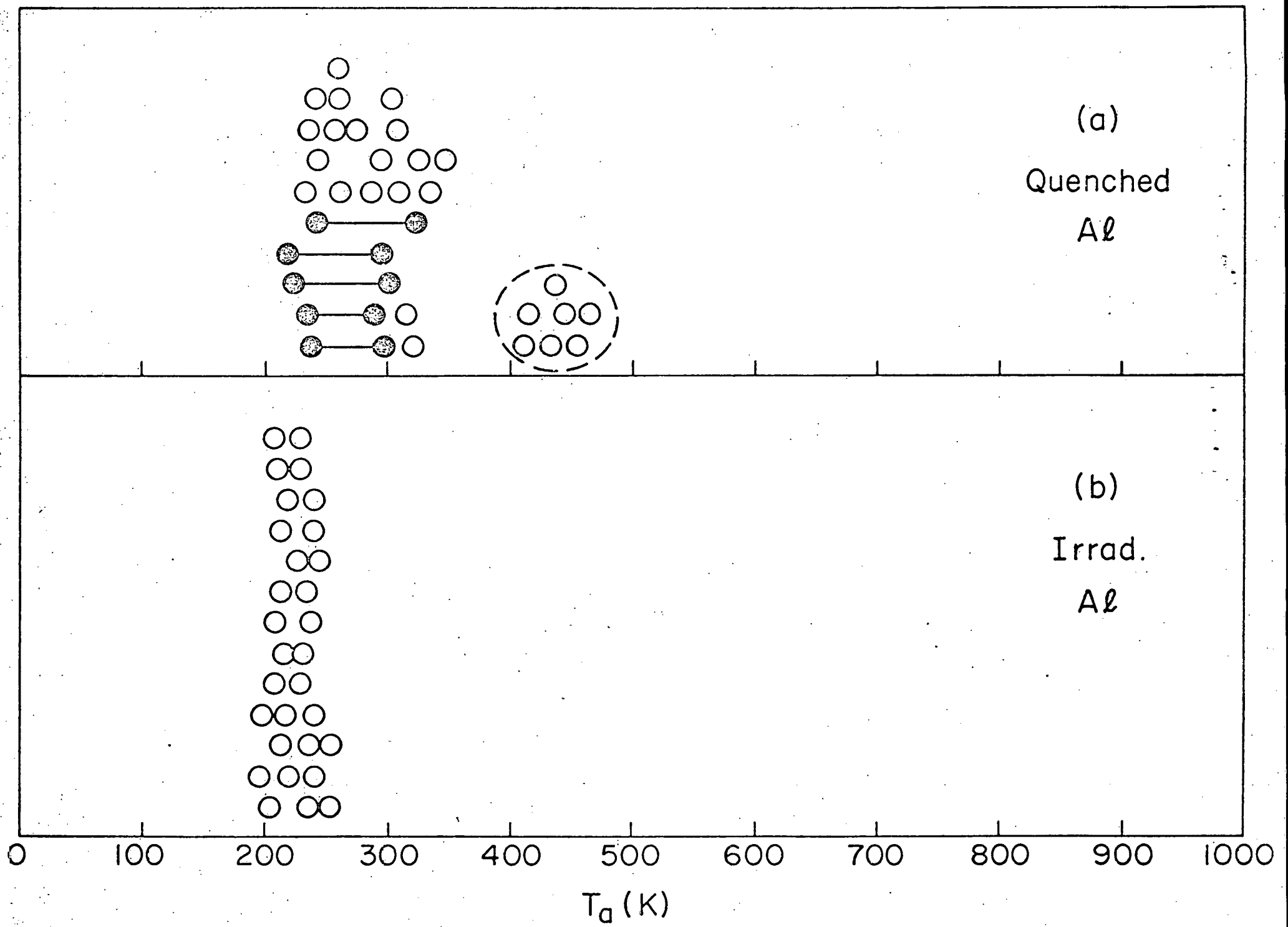
(a)
Quenched
Al
(b)
Irrad.
Al
0
100
200
300
400
500
600
700
800
900
1000
T_a (K)

FIG 5

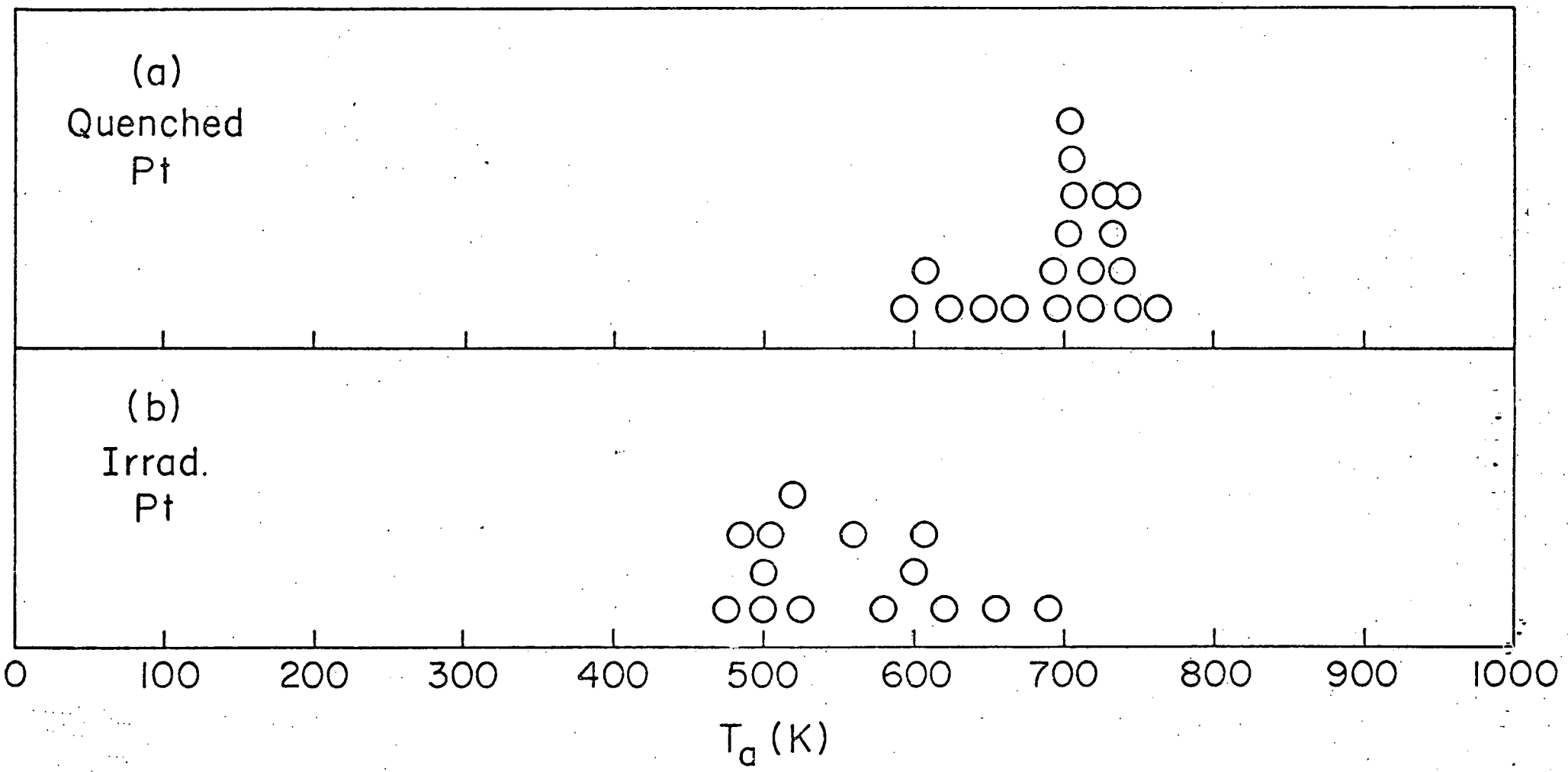
(a)
Quenched
Pt
(b)
Irrad.
Pt
0
100
200
300
400
500
600
700
800
900
1000
T_a (K)

FIG 6

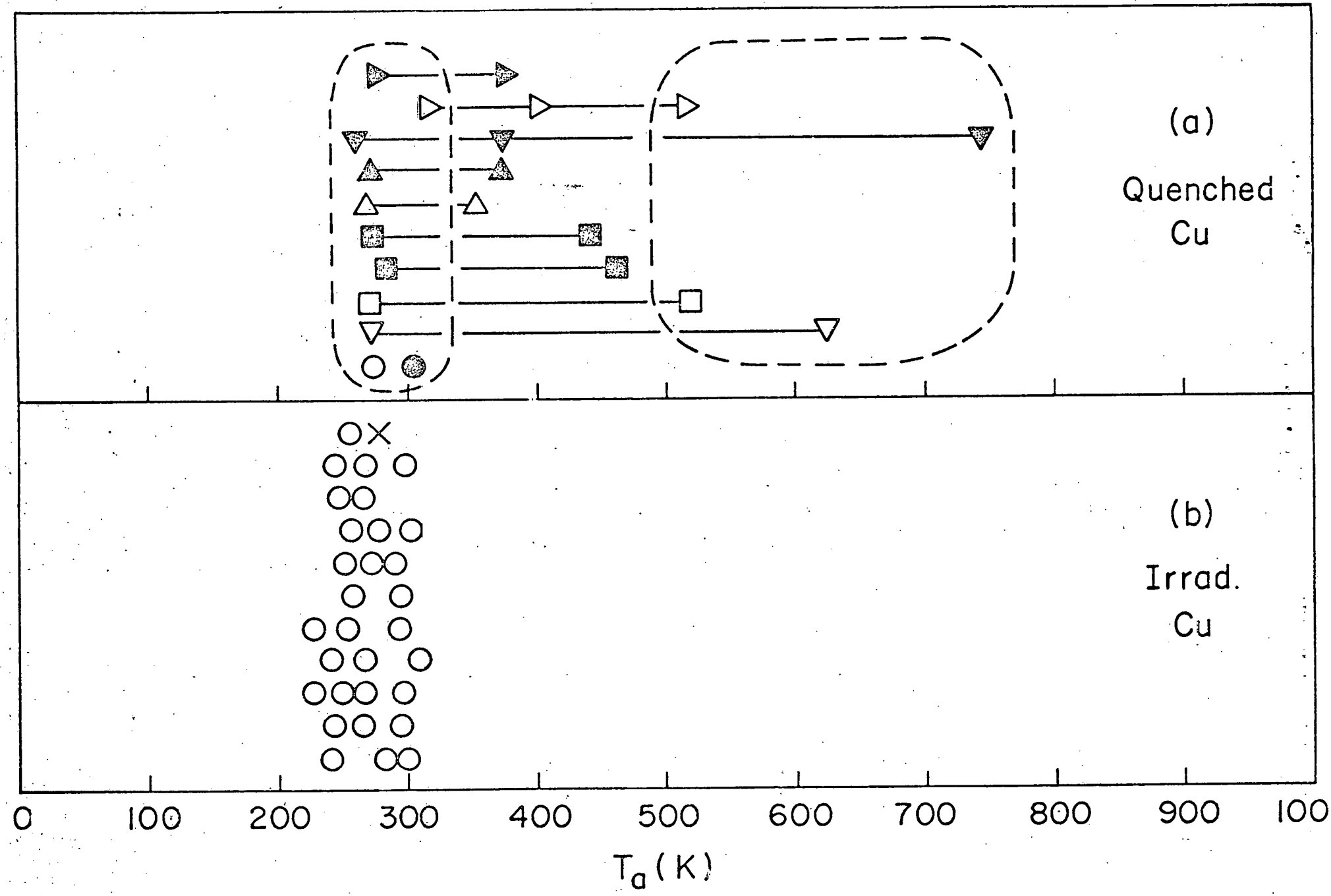
(a)
Quenched
Cu
(b)
Irrad.
Cu
0
100
200
300
400
500
600
700
800
900
1000
T_a (K)

FIG

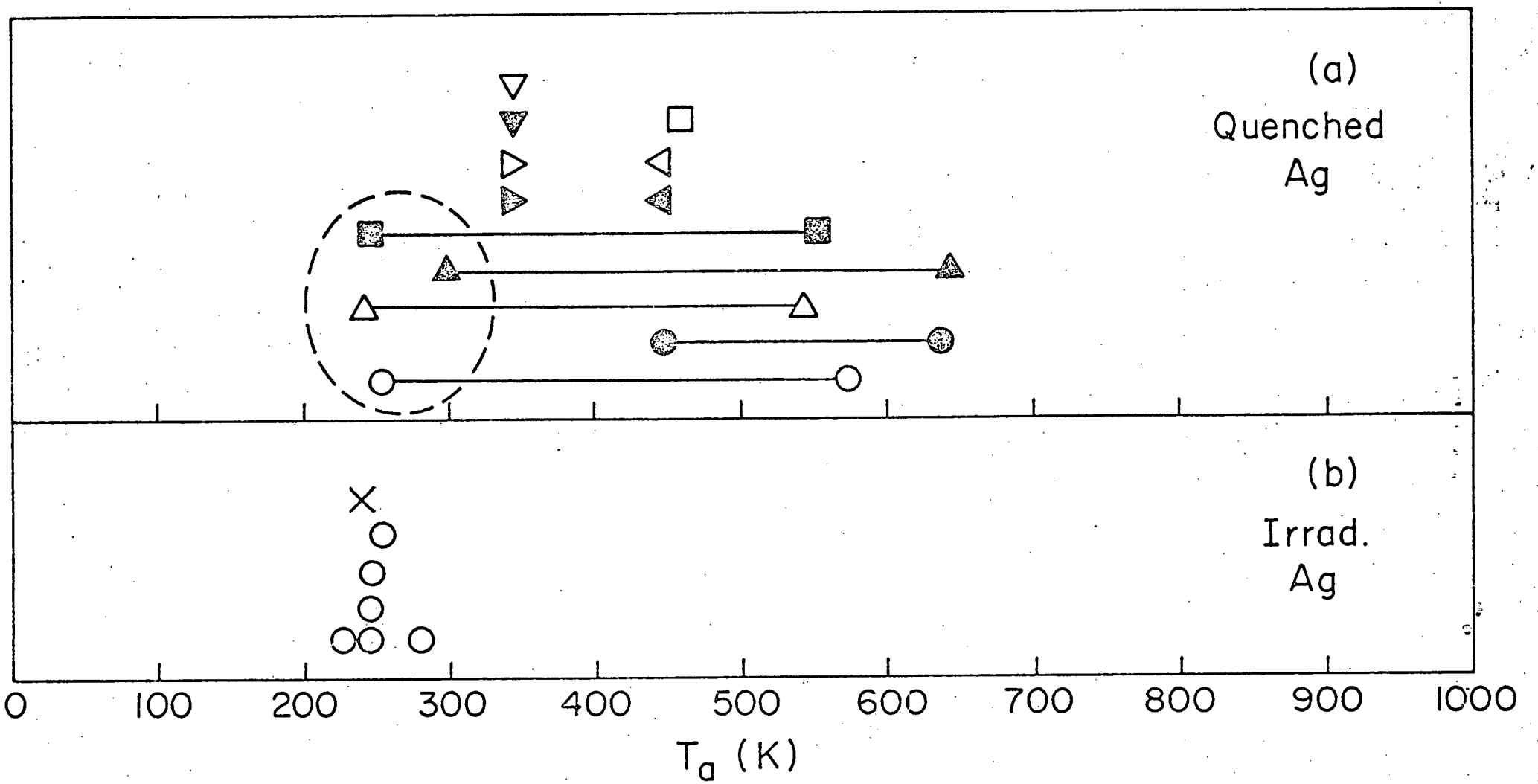
(a)
Quenched
Ag
(b)
Irrad.
Ag
0
100
200
300
400
500
600
700
800
900
1000
T_a (K)

FIG. 8

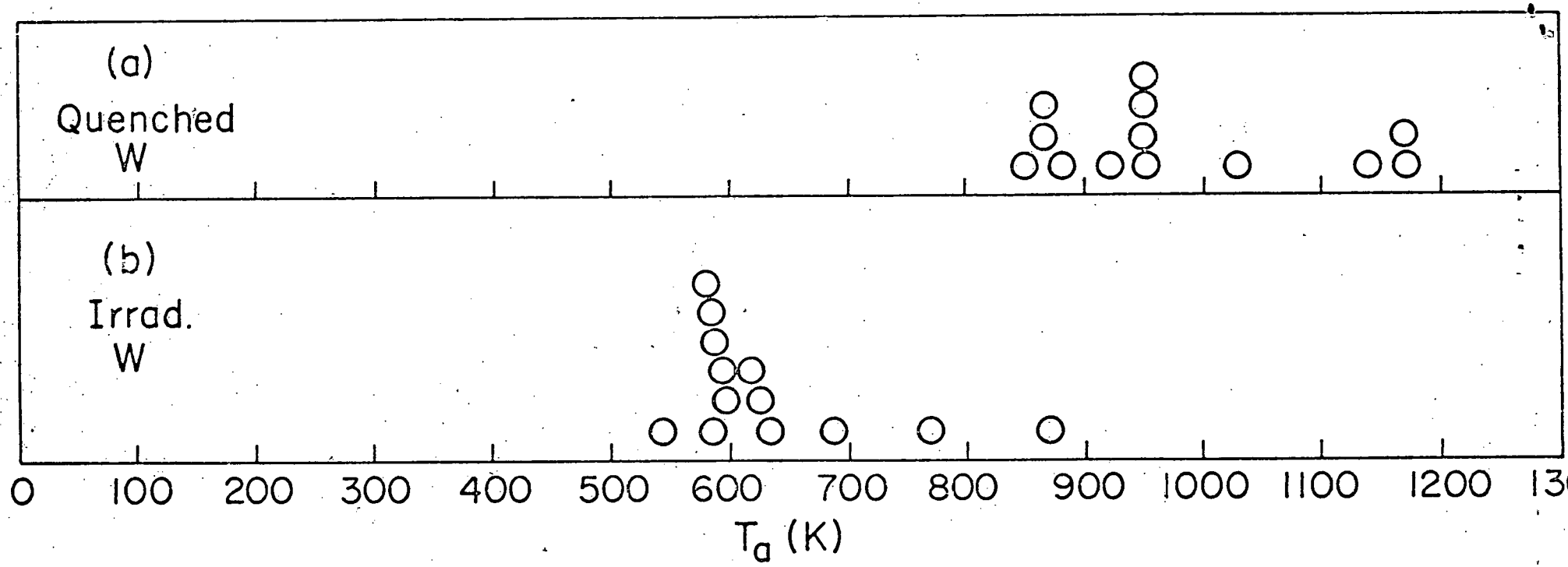
(a)
Quenched
W
(b)
Irrad.
W
0
100
200
300
400
500
600
700
800
900
1000
1100
1200
1300
T_a (K)

FIG 9

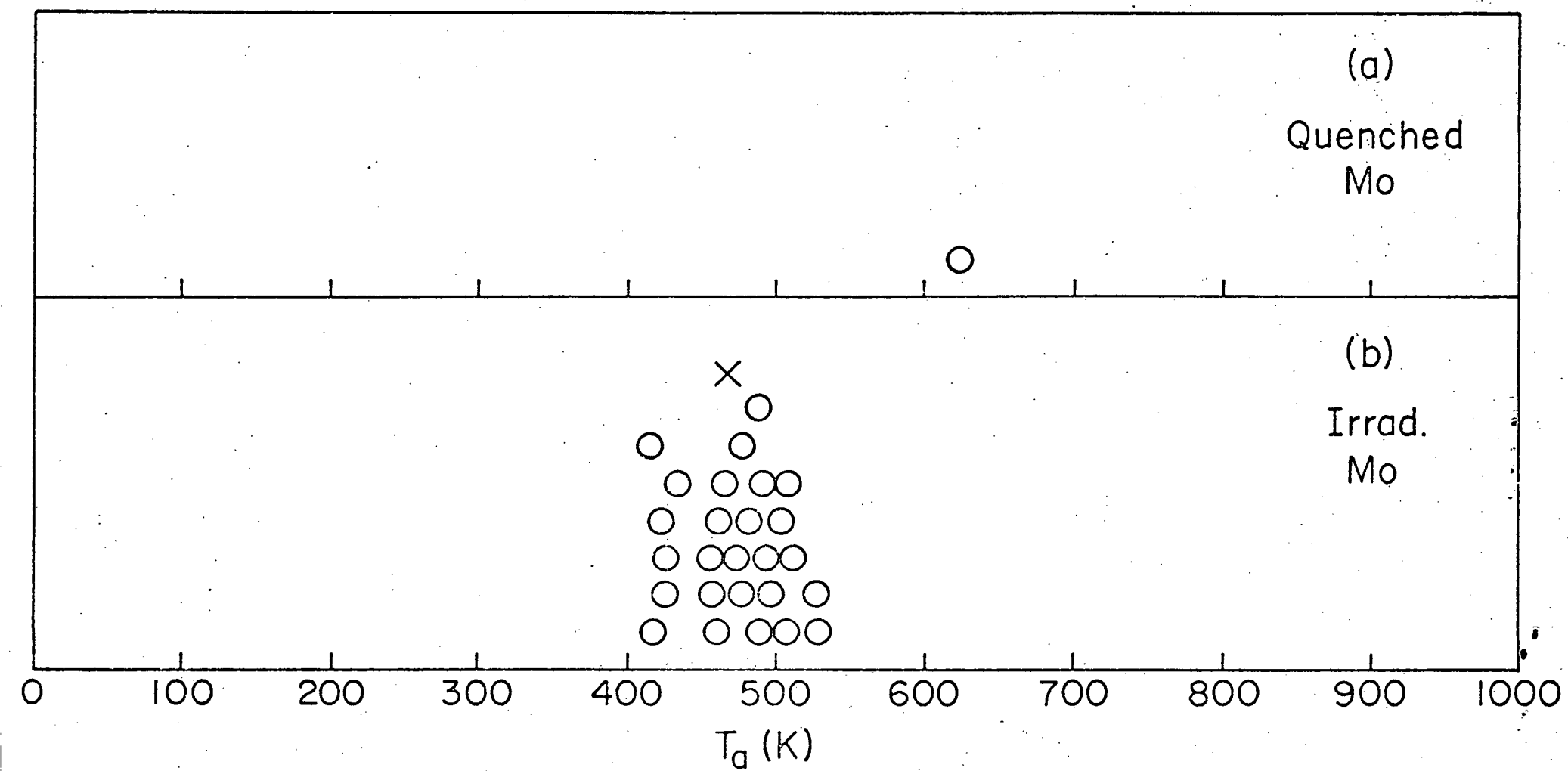
(a)
Quenched
Mo
(b)
Irrad.
Mo
0
100
200
300
400
500
600
700
800
900
1000
T_a (K)

FIG. 10

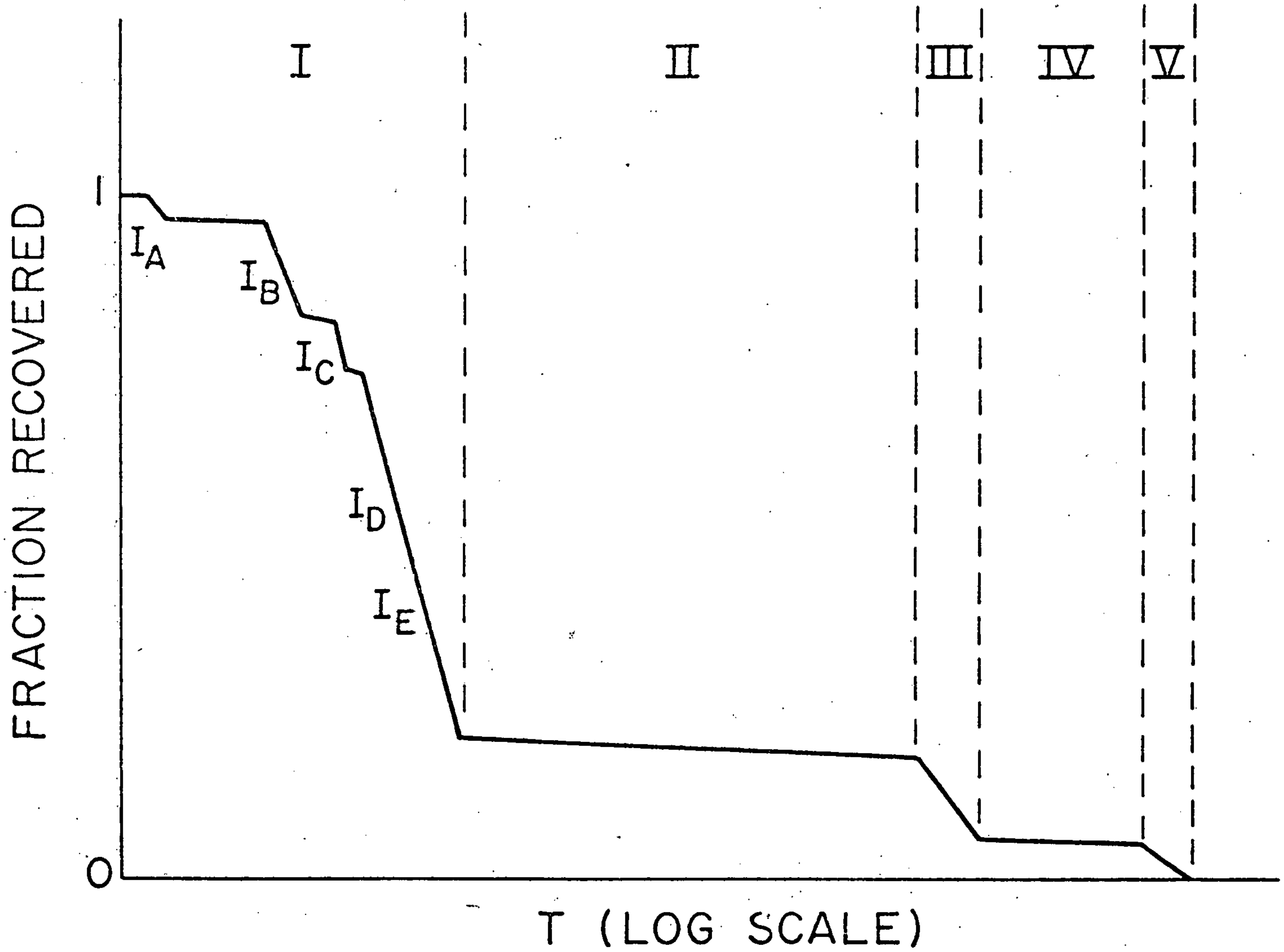

FIG 11

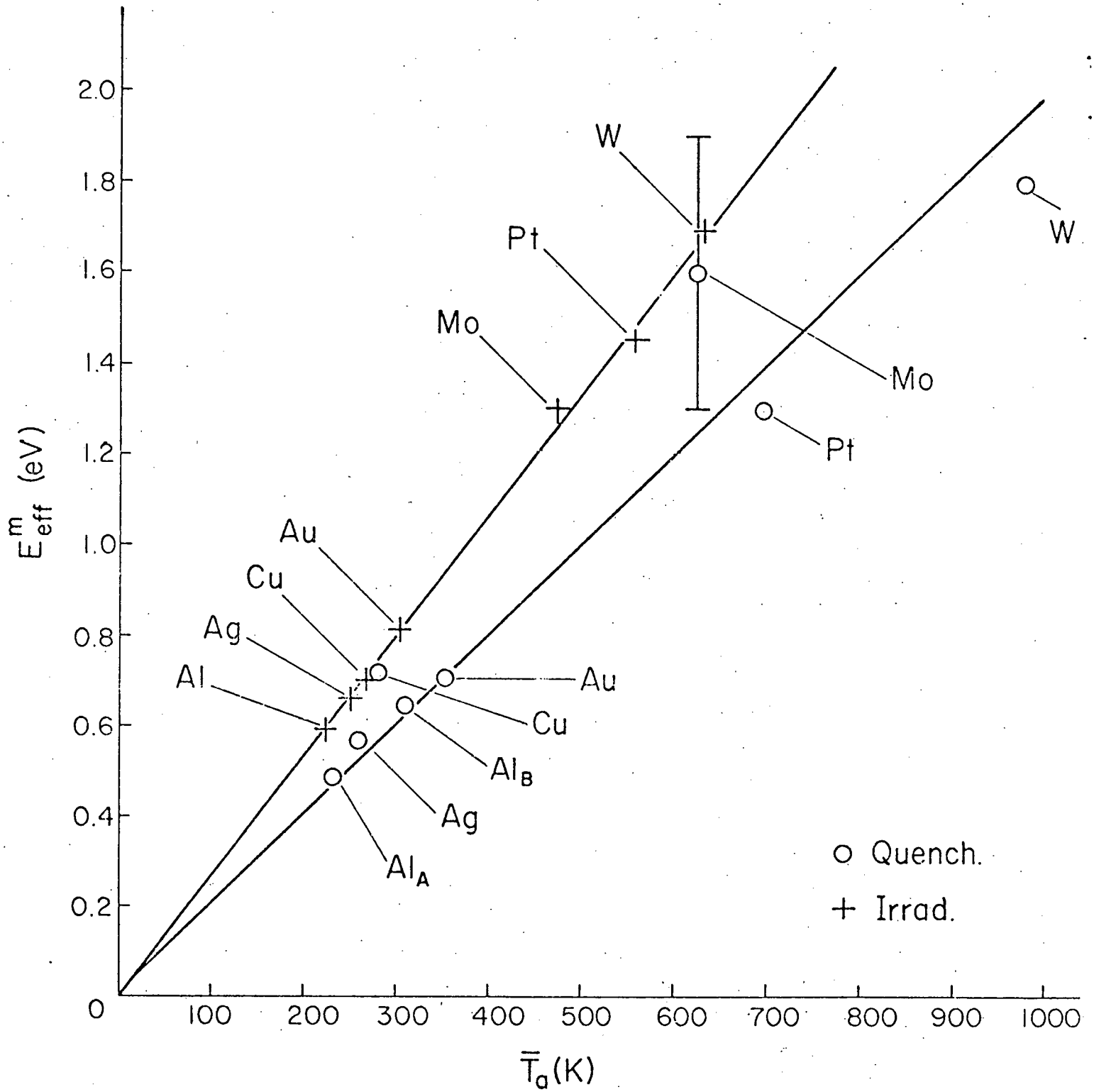
2.0
1.8
1.6
1.4
1.2
1.0
0.8
0.6
0.4
0.2
0
E^m_{eff} (eV)
100
200
300
400
500
600
700
800
900
1000
$\bar{T}_a$(K)
W
Pt
Mo
Mo
W
Pt
Au
Cu
Ag
Al
Au
Cu
Al_B
Ag
Al_A
O Quench.
+ Irrad.

FIG 12